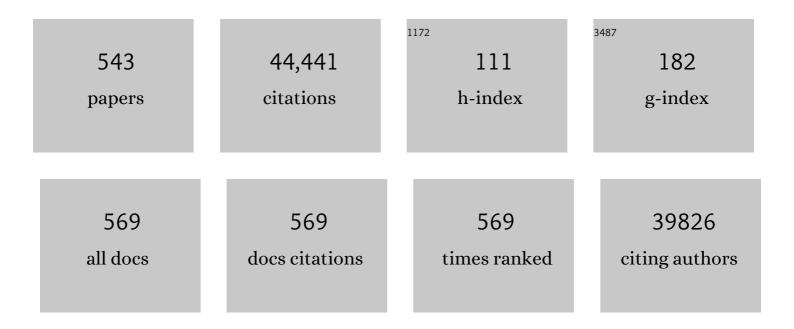
List of Publications by Year in descending order

Source: https://exaly.com/author-pdf/6812871/publications.pdf Version: 2024-02-01



ΥλΝΗ ΖΗΛΟ

#	Article	IF	CITATIONS
1	Biomedical Applications of Supramolecular Systems Based on Host–Guest Interactions. Chemical Reviews, 2015, 115, 7794-7839.	47.7	980
2	Ultrathin 2D Metal–Organic Framework Nanosheets. Advanced Materials, 2015, 27, 7372-7378.	21.0	943
3	Covalent Organic Frameworks for CO2Capture. Advanced Materials, 2016, 28, 2855-2873.	21.0	873
4	Pseudocapacitive Na-Ion Storage Boosts High Rate and Areal Capacity of Self-Branched 2D Layered Metal Chalcogenide Nanoarrays. ACS Nano, 2016, 10, 10211-10219.	14.6	844
5	Versatile Polydopamine Platforms: Synthesis and Promising Applications for Surface Modification and Advanced Nanomedicine. ACS Nano, 2019, 13, 8537-8565.	14.6	670
6	Noncovalent Functionalization of Single-Walled Carbon Nanotubes. Accounts of Chemical Research, 2009, 42, 1161-1171.	15.6	654
7	Mechanized Silica Nanoparticles: A New Frontier in Theranostic Nanomedicine. Accounts of Chemical Research, 2011, 44, 903-913.	15.6	584
8	Autonomous in Vitro Anticancer Drug Release from Mesoporous Silica Nanoparticles by pH-Sensitive Nanovalves. Journal of the American Chemical Society, 2010, 132, 12690-12697.	13.7	550
9	Charge-Convertible Carbon Dots for Imaging-Guided Drug Delivery with Enhanced <i>in Vivo</i> Cancer Therapeutic Efficiency. ACS Nano, 2016, 10, 4410-4420.	14.6	543
10	Heterogeneous Catalysis in Zeolites, Mesoporous Silica, and Metal–Organic Frameworks. Advanced Materials, 2017, 29, 1701139.	21.0	522
11	Ultralong room temperature phosphorescence from amorphous organic materials toward confidential information encryption and decryption. Science Advances, 2018, 4, eaas9732.	10.3	515
12	A Triazole-Containing Metal–Organic Framework as a Highly Effective and Substrate Size-Dependent Catalyst for CO <sub>2</sub> Conversion. Journal of the American Chemical Society, 2016, 138, 2142-2145.	13.7	504
13	Light-Operated Mechanized Nanoparticles. Journal of the American Chemical Society, 2009, 131, 1686-1688.	13.7	482
14	Graphene-Based Microbots for Toxic Heavy Metal Removal and Recovery from Water. Nano Letters, 2016, 16, 2860-2866.	9.1	473
15	A p-type Ti( <scp>iv</scp> )-based metal–organic framework with visible-light photo-response. Chemical Communications, 2014, 50, 3786-3788.	4.1	424
16	Ultrathin ZnIn <sub>2</sub> S <sub>4</sub> Nanosheets Anchored on Ti <sub>3</sub> C <sub>2</sub> T <sub><i>X</i></sub> MXene for Photocatalytic H <sub>2</sub> Evolution. Angewandte Chemie - International Edition, 2020, 59, 11287-11292.	13.8	416
17	Nanoscale covalent organic frameworks as smart carriers for drug delivery. Chemical Communications, 2016, 52, 4128-4131.	4.1	384
18	Carbon Quantum Dot Implanted Graphite Carbon Nitride Nanotubes: Excellent Charge Separation and Enhanced Photocatalytic Hydrogen Evolution. Angewandte Chemie - International Edition, 2018, 57, 5765-5771.	13.8	372

#	Article	IF	CITATIONS
19	Docking in Metal-Organic Frameworks. Science, 2009, 325, 855-859.	12.6	360
20	Self-assembled single-atom nanozyme for enhanced photodynamic therapy treatment of tumor. Nature Communications, 2020, 11, 357.	12.8	339
21	Azobenzene-Based Light-Responsive Hydrogel System. Langmuir, 2009, 25, 8442-8446.	3.5	325
22	Molecular Engineering for Metalâ€Free Amorphous Materials with Roomâ€Temperature Phosphorescence. Angewandte Chemie - International Edition, 2020, 59, 11206-11216.	13.8	322
23	Metal–Organic Framework Derived Nanozymes in Biomedicine. Accounts of Chemical Research, 2020, 53, 1389-1400.	15.6	308
24	Integrating Suitable Linkage of Covalent Organic Frameworks into Covalently Bridged Inorganic/Organic Hybrids toward Efficient Photocatalysis. Journal of the American Chemical Society, 2020, 142, 4862-4871.	13.7	304
25	pH-Operated Nanopistons on the Surfaces of Mesoporous Silica Nanoparticles. Journal of the American Chemical Society, 2010, 132, 13016-13025.	13.7	296
26	Catalase-Integrated Hyaluronic Acid as Nanocarriers for Enhanced Photodynamic Therapy in Solid Tumor. ACS Nano, 2019, 13, 4742-4751.	14.6	293
27	Functional Mesoporous Silica Nanoparticles for Photothermalâ€Controlled Drug Delivery Inâ€Vivo. Angewandte Chemie - International Edition, 2012, 51, 8373-8377.	13.8	290
28	Solutions to the Drawbacks of Photothermal and Photodynamic Cancer Therapy. Advanced Science, 2021, 8, 2002504.	11.2	285
29	A Mesoporous Nanoenzyme Derived from Metal–Organic Frameworks with Endogenous Oxygen Generation to Alleviate Tumor Hypoxia for Significantly Enhanced Photodynamic Therapy. Advanced Materials, 2019, 31, e1901893.	21.0	282
30	Multifunctional Mesoporous Silica Nanoparticles for Cancerâ€Targeted and Controlled Drug Delivery. Advanced Functional Materials, 2012, 22, 5144-5156.	14.9	281
31	Color-tunable ultralong organic room temperature phosphorescence from a multicomponent copolymer. Nature Communications, 2020, 11, 944.	12.8	278
32	Covalent Organic Frameworks Formed with Two Types of Covalent Bonds Based on Orthogonal Reactions. Journal of the American Chemical Society, 2015, 137, 1020-1023.	13.7	276
33	Degradability and Clearance of Inorganic Nanoparticles for Biomedical Applications. Advanced Materials, 2019, 31, e1805730.	21.0	267
34	A Hypoxiaâ€Responsive Albuminâ€Based Nanosystem for Deep Tumor Penetration and Excellent Therapeutic Efficacy. Advanced Materials, 2019, 31, e1901513.	21.0	263
35	Pillararene-based self-assembled amphiphiles. Chemical Society Reviews, 2018, 47, 5491-5528.	38.1	258
36	Controlling Supramolecular Chirality in Multicomponent Self-Assembled Systems. Accounts of Chemical Research, 2018, 51, 2324-2334.	15.6	255

#	Article	IF	CITATIONS
37	Immobilizing Gold Nanoparticles in Mesoporous Silica Covered Reduced Graphene Oxide: A Hybrid Material for Cancer Cell Detection through Hydrogen Peroxide Sensing. ACS Applied Materials & Interfaces, 2014, 6, 13648-13656.	8.0	253
38	Lithiation-induced amorphization of Pd3P2S8 for highly efficient hydrogen evolution. Nature Catalysis, 2018, 1, 460-468.	34.4	247
39	Titanium-based metal–organic frameworks for photocatalytic applications. Coordination Chemistry Reviews, 2018, 359, 80-101.	18.8	246
40	Excitationâ€Dependent Longâ€Life Luminescent Polymeric Systems under Ambient Conditions. Angewandte Chemie - International Edition, 2020, 59, 9967-9971.	13.8	242
41	Biocompatible, Uniform, and Redispersible Mesoporous Silica Nanoparticles for Cancerâ€Targeted Drug Delivery In Vivo. Advanced Functional Materials, 2014, 24, 2450-2461.	14.9	238
42	Supramolecular Adhesive Hydrogels for Tissue Engineering Applications. Chemical Reviews, 2022, 122, 5604-5640.	47.7	238
43	Large-Area, Flexible, Transparent, and Long-Lived Polymer-Based Phosphorescence Films. Journal of the American Chemical Society, 2021, 143, 13675-13685.	13.7	237
44	A Preloaded Amorphous Calcium Carbonate/Doxorubicin@Silica Nanoreactor for pHâ€Responsive Delivery of an Anticancer Drug. Angewandte Chemie - International Edition, 2015, 54, 919-922.	13.8	222
45	Biocompatible Pillararene-Assembly-Based Carriers for Dual Bioimaging. ACS Nano, 2013, 7, 7853-7863.	14.6	219
46	Engineering a Hollow Nanocontainer Platform with Multifunctional Molecular Machines for Tumor-Targeted Therapy <i>in Vitro</i> and <i>in Vivo</i> . ACS Nano, 2013, 7, 10271-10284.	14.6	212
47	Pillarareneâ€Based Assemblies: Design Principle, Preparation and Applications. Chemistry - A European Journal, 2013, 19, 16862-16879.	3.3	202
48	Tumor microenvironment-activatable Fe-doxorubicin preloaded amorphous CaCO <sub>3</sub> nanoformulation triggers ferroptosis in target tumor cells. Science Advances, 2020, 6, eaax1346.	10.3	200
49	Polymer-Coated Hollow Mesoporous Silica Nanoparticles for Triple-Responsive Drug Delivery. ACS Applied Materials & Interfaces, 2015, 7, 18179-18187.	8.0	198
50	Ultrasmall Phosphorescent Polymer Dots for Ratiometric Oxygen Sensing and Photodynamic Cancer Therapy. Advanced Functional Materials, 2014, 24, 4823-4830.	14.9	197
51	Ultraviolet irradiation-responsive dynamic ultralong organic phosphorescence in polymeric systems. Nature Communications, 2021, 12, 2297.	12.8	196
52	Photoresponsive Luminescent Polymeric Hydrogels for Reversible Information Encryption and Decryption. Advanced Science, 2019, 6, 1901529.	11.2	193
53	Graphene Oxide Wrapping on Squaraine-Loaded Mesoporous Silica Nanoparticles for Bioimaging. Journal of the American Chemical Society, 2012, 134, 17346-17349.	13.7	188
54	HCAR1/MCT1 Regulates Tumor Ferroptosis through the Lactate-Mediated AMPK-SCD1 Activity and Its Therapeutic Implications. Cell Reports, 2020, 33, 108487.	6.4	179

#	Article	IF	CITATIONS
55	Dual-Responsive Carbon Dots for Tumor Extracellular Microenvironment Triggered Targeting and Enhanced Anticancer Drug Delivery. ACS Applied Materials & Interfaces, 2016, 8, 18732-18740.	8.0	178
56	Hierarchical Porous LiNi1/3Co1/3Mn1/3O2 Nano-/Micro Spherical Cathode Material: Minimized Cation Mixing and Improved Li+ Mobility for Enhanced Electrochemical Performance. Scientific Reports, 2016, 6, 25771.	3.3	178
57	Recent advancements of graphene in biomedicine. Journal of Materials Chemistry B, 2013, 1, 2542.	5.8	176
58	Colorâ€Tunable Polymeric Longâ€Persistent Luminescence Based on Polyphosphazenes. Advanced Materials, 2020, 32, e1907355.	21.0	176
59	Cancer Cell Detection and Therapeutics Using Peroxidase-Active Nanohybrid of Gold Nanoparticle-Loaded Mesoporous Silica-Coated Graphene. ACS Applied Materials & Interfaces, 2015, 7, 9807-9816.	8.0	171
60	Lightâ€Induced Charge Transfer in Pyrene/CdSeâ€&WNT Hybrids. Advanced Materials, 2008, 20, 939-946.	21.0	165
61	Controlling Supramolecular Chirality of Two-Component Hydrogels by <i>J</i> - and <i>H</i> -Aggregation of Building Blocks. Journal of the American Chemical Society, 2018, 140, 6467-6473.	13.7	165
62	Cyanostilbene-based intelligent organic optoelectronic materials. Journal of Materials Chemistry C, 2013, 1, 1059-1065.	5.5	162
63	Integrated Hollow Mesoporous Silica Nanoparticles for Target Drug/siRNA Coâ€Delivery. Chemistry - A European Journal, 2013, 19, 15593-15603.	3.3	160
64	Photoresponsive supramolecular coordination polyelectrolyte as smart anticounterfeiting inks. Nature Communications, 2021, 12, 1363.	12.8	160
65	Upconversion Nanoparticles as a Contrast Agent for Photoacoustic Imaging in Live Mice. Advanced Materials, 2014, 26, 5633-5638.	21.0	158
66	Stimulated Release of Sizeâ€5elected Cargos in Succession from Mesoporous Silica Nanoparticles. Angewandte Chemie - International Edition, 2012, 51, 5460-5465.	13.8	157
67	Room-temperature synthesis of bimetallic Co–Zn based zeolitic imidazolate frameworks in water for enhanced CO <sub>2</sub> and H <sub>2</sub> uptakes. Journal of Materials Chemistry A, 2016, 4, 14932-14938.	10.3	156
68	Versatile bimetallic lanthanide metal-organic frameworks for tunable emission and efficient fluorescence sensing. Communications Chemistry, 2018, 1, .	4.5	156
69	Selfâ€Assembled Singleâ€Site Nanozyme for Tumorâ€Specific Amplified Cascade Enzymatic Therapy. Angewandte Chemie - International Edition, 2021, 60, 3001-3007.	13.8	156
70	Multifunctional Nanoparticles Selfâ€Assembled from Small Organic Building Blocks for Biomedicine. Advanced Materials, 2016, 28, 7304-7339.	21.0	155
71	Long-Lived Organic Room-Temperature Phosphorescence from Amorphous Polymer Systems. Accounts of Chemical Research, 2022, 55, 1160-1170.	15.6	155
72	An Ultrasmall SnFe <sub>2</sub> O <sub>4</sub> Nanozyme with Endogenous Oxygen Generation and Glutathione Depletion for Synergistic Cancer Therapy. Advanced Functional Materials, 2021, 31, 2006216.	14.9	154

#	Article	IF	CITATIONS
73	ZnO–DOX@ZIF-8 Core–Shell Nanoparticles for pH-Responsive Drug Delivery. ACS Biomaterials Science and Engineering, 2017, 3, 2223-2229.	5.2	151
74	Guiding Transition Metalâ€Ðoped Hollow Cerium Tandem Nanozymes with Elaborately Regulated Multiâ€Enzymatic Activities for Intensive Chemodynamic Therapy. Advanced Materials, 2022, 34, e2107054.	21.0	150
75	A Vanadyl Complex Grafted to Periodic Mesoporous Organosilica: A Green Catalyst for Selective Hydroxylation of Benzene to Phenol. Angewandte Chemie - International Edition, 2012, 51, 7756-7761.	13.8	149
76	Two fully conjugated covalent organic frameworks as anode materials for lithium ion batteries. Journal of Materials Chemistry A, 2016, 4, 14106-14110.	10.3	149
77	Achieving Amorphous Ultralong Room Temperature Phosphorescence by Coassembling Planar Small Organic Molecules with Polyvinyl Alcohol. Advanced Functional Materials, 2019, 29, 1807243.	14.9	147
78	Direct Z-scheme TiO2–ZnIn2S4 nanoflowers for cocatalyst-free photocatalytic water splitting. Applied Catalysis B: Environmental, 2021, 291, 120126.	20.2	147
79	Near-Infrared Squaraine Dye Encapsulated Micelles for <i>in Vivo</i> Fluorescence and Photoacoustic Bimodal Imaging. ACS Nano, 2015, 9, 5695-5704.	14.6	145
80	Nitrogenâ€Doped Carbonâ€Coated CuOâ€In <sub>2</sub> O <sub>3</sub> p–n Heterojunction for Remarkable Photocatalytic Hydrogen Evolution. Advanced Energy Materials, 2019, 9, 1902839.	<sup>2</sup> 19.5	145
81	Unimolecular Photoconversion of Multicolor Luminescence on Hierarchical Self-Assemblies. Journal of the American Chemical Society, 2013, 135, 5175-5182.	13.7	144
82	Polymeric Rotaxane Constructed from the Inclusion Complex of β-Cyclodextrin and 4,4′-Dipyridine by Coordination with Nickel(II) Ions. Angewandte Chemie - International Edition, 2003, 42, 3260-3263.	13.8	143
83	Halogen-Assisted Piezochromic Supramolecular Assemblies for Versatile Haptic Memory. Journal of the American Chemical Society, 2017, 139, 436-441.	13.7	142
84	Surfactant Media To Grow New Crystalline Cobalt 1,3,5-Benzenetricarboxylate Metal–Organic Frameworks. Inorganic Chemistry, 2014, 53, 8529-8537.	4.0	140
85	Graphene oxide wrapped gold nanoparticles for intracellular Raman imaging and drug delivery. Journal of Materials Chemistry B, 2013, 1, 6495.	5.8	139
86	Intracellular redox-activated anticancer drug delivery by functionalized hollow mesoporous silica nanoreservoirs with tumor specificity. Biomaterials, 2014, 35, 7951-7962.	11.4	134
87	Structural Engineering of Luminogens with High Emission Efficiency Both in Solution and in the Solid State. Angewandte Chemie - International Edition, 2019, 58, 11419-11423.	13.8	133
88	NIRâ€Lightâ€Activated Combination Therapy with a Precise Ratio of Photosensitizer and Prodrug Using a Host–Guest Strategy. Angewandte Chemie - International Edition, 2019, 58, 7641-7646.	13.8	133
89	Crossâ€Linked Polyphosphazene Hollow Nanosphereâ€Derived N/Pâ€Doped Porous Carbon with Single Nonprecious Metal Atoms for the Oxygen Reduction Reaction. Angewandte Chemie - International Edition, 2020, 59, 14639-14646.	13.8	133
90	A Redox-Switchable α-Cyclodextrin-Based [2]Rotaxane. Journal of the American Chemical Society, 2008, 130, 11294-11296.	13.7	132

#	Article	IF	CITATIONS
91	Circularly Polarized Organic Room Temperature Phosphorescence from Amorphous Copolymers. Journal of the American Chemical Society, 2021, 143, 18527-18535.	13.7	132
92	Selective H <sub>2</sub> S/CO <sub>2</sub> Separation by Metal–Organic Frameworks Based on Chemical-Physical Adsorption. Journal of Physical Chemistry C, 2017, 121, 13249-13255.	3.1	131
93	Engineered Hybrid Nanoparticles for On-Demand Diagnostics and Therapeutics. Accounts of Chemical Research, 2015, 48, 3016-3025.	15.6	130
94	Amorphous Ionic Polymers with Colorâ€Tunable Ultralong Organic Phosphorescence. Angewandte Chemie - International Edition, 2019, 58, 18776-18782.	13.8	129
95	A Lightâ€Stimulated Molecular Switch Driven by Radical–Radical Interactions in Water. Angewandte Chemie - International Edition, 2011, 50, 6782-6788.	13.8	127
96	Covalent-Organic-Framework-Based Composite Materials. CheM, 2020, 6, 3172-3202.	11.7	127
97	Synthesis, Characterization, and Nonâ€Volatile Memory Device Application of an Nâ€Substituted Heteroacene. Chemistry - an Asian Journal, 2014, 9, 779-783.	3.3	123
98	Organogel Formation by a Cholesterol-Stoppered Bistable [2]Rotaxane and Its Dumbbell Precursor. Journal of the American Chemical Society, 2008, 130, 6348-6350.	13.7	122
99	A Rationally Designed Nitrogen-Rich Metal-Organic Framework and Its Exceptionally High CO2 and H2 Uptake Capability. Scientific Reports, 2013, 3, 1149.	3.3	122
100	Bimetallic Metalâ€Organic Frameworks: Probing the Lewis Acid Site for CO <sub>2</sub> Conversion. Small, 2016, 12, 2334-2343.	10.0	122
101	Enhancing Organic Phosphorescence by Manipulating Heavy-Atom Interaction. Crystal Growth and Design, 2016, 16, 808-813.	3.0	122
102	Synthesis and Physical Properties of Four Hexazapentacene Derivatives. Journal of the American Chemical Society, 2012, 134, 20298-20301.	13.7	121
103	Kinetically Controlling Phase Transformations of Crystalline Mercury Selenidostannates through Surfactant Media. Inorganic Chemistry, 2013, 52, 4148-4150.	4.0	121
104	Microneedle-Assisted Topical Delivery of Photodynamically Active Mesoporous Formulation for Combination Therapy of Deep-Seated Melanoma. ACS Nano, 2018, 12, 11936-11948.	14.6	121
105	Targeted Delivery of 5-Aminolevulinic Acid by Multifunctional Hollow Mesoporous Silica Nanoparticles for Photodynamic Skin Cancer Therapy. ACS Applied Materials & Interfaces, 2015, 7, 10671-10676.	8.0	120
106	Three-Dimensional Porous Graphene Networks and Hybrids for Lithium-Ion Batteries and Supercapacitors. CheM, 2017, 2, 171-200.	11.7	119
107	Highly Effective Carbon Fixation via Catalytic Conversion of CO <sub>2</sub> by an Acylamide-Containing Metal–Organic Framework. Chemistry of Materials, 2017, 29, 9256-9261.	6.7	116
108	Integrated graphene/nanoparticle hybrids for biological and electronic applications. Nanoscale, 2014, 6, 6245-6266.	5.6	114

#	Article	IF	CITATIONS
109	Emerging Applications of Metal–Organic Frameworks and Covalent Organic Frameworks. Chemistry of Materials, 2016, 28, 8079-8081.	6.7	114
110	Targeted delivery of doxorubicin to mitochondria using mesoporous silica nanoparticle nanocarriers. Nanoscale, 2015, 7, 16677-16686.	5.6	113
111	Selective wet-chemical etching to create TiO2@MOF frame heterostructure for efficient photocatalytic hydrogen evolution. Nano Energy, 2020, 74, 104909.	16.0	113
112	Relative Unidirectional Translation in an Artificial Molecular Assembly Fueled by Light. Journal of the American Chemical Society, 2013, 135, 18609-18620.	13.7	112
113	NIRâ€Actuated Remote Activation of Ferroptosis in Target Tumor Cells through a Photothermally Responsive Ironâ€Chelated Biopolymer Nanoplatform. Angewandte Chemie - International Edition, 2021, 60, 8938-8947.	13.8	112
114	Applications of Light-Responsive Systems for Cancer Theranostics. ACS Applied Materials & Interfaces, 2018, 10, 21021-21034.	8.0	111
115	Experimental and Theoretical Investigation of Mesoporous MnO <sub>2</sub> Nanosheets with Oxygen Vacancies for High-Efficiency Catalytic DeNO <sub><i>x</i></sub> . ACS Catalysis, 2018, 8, 3865-3874.	11.2	111
116	Ultrasmall Alloy Nanozyme for Ultrasound- and Near-Infrared Light-Promoted Tumor Ablation. ACS Nano, 2021, 15, 7774-7782.	14.6	111
117	Approaching a stable, green twisted heteroacene through "clean reaction―strategy. Chemical Communications, 2012, 48, 5974.	4.1	110
118	Control on Dimensions and Supramolecular Chirality of Self-Assemblies through Light and Metal Ions. Journal of the American Chemical Society, 2018, 140, 16275-16283.	13.7	110
119	Room-Temperature Chemoselective Reduction of Nitro Groups Using Non-noble Metal Nanocatalysts in Water. Inorganic Chemistry, 2014, 53, 2904-2909.	4.0	109
120	Size-Dependent Catalytic Activity of Palladium Nanoparticles Fabricated in Porous Organic Polymers for Alkene Hydrogenation at Room Temperature. ACS Applied Materials & Interfaces, 2016, 8, 15307-15319.	8.0	109
121	Reduction-sensitive fluorescence enhanced polymeric prodrug nanoparticles for combinational photothermal-chemotherapy. Biomaterials, 2018, 163, 14-24.	11.4	109
122	Bioengineering of Metal-organic Frameworks for Nanomedicine. Theranostics, 2019, 9, 3122-3133.	10.0	108
123	Significant gas uptake enhancement by post-exchange of zinc(ii) with copper(ii) within a metal–organic framework. Chemical Communications, 2012, 48, 10286.	4.1	107
124	Renalâ€Clearable Nickelâ€Doped Carbon Dots with Boosted Photothermal Conversion Efficiency for Multimodal Imagingâ€Guided Cancer Therapy in the Second Nearâ€Infrared Biowindow. Advanced Functional Materials, 2021, 31, 2100549.	14.9	107
125	Double-shelled hollow rods assembled from nitrogen/sulfur-codoped carbon coated indium oxide nanoparticles as excellent photocatalysts. Nature Communications, 2019, 10, 2270.	12.8	105
126	Cross-Linked Polyphosphazene Nanospheres Boosting Long-Lived Organic Room-Temperature Phosphorescence. Journal of the American Chemical Society, 2022, 144, 6107-6117.	13.7	105

#	Article	IF	CITATIONS
127	General and Robust Photothermalâ€Heatingâ€Enabled Highâ€Efficiency Photoelectrochemical Water Splitting. Advanced Materials, 2021, 33, e2004406.	21.0	104
128	Nitrogenâ€Rich Porous Adsorbents for CO <sub>2</sub> Capture and Storage. Chemistry - an Asian Journal, 2013, 8, 1680-1691.	3.3	103
129	Macrocycle-based metal-organic frameworks. Coordination Chemistry Reviews, 2015, 292, 74-90.	18.8	103
130	Strategies for enhancing cancer chemodynamic therapy performance. Exploration, 2022, 2, .	11.0	103
131	Perylene-Derived Single-Component Organic Nanoparticles with Tunable Emission: Efficient Anticancer Drug Carriers with Real-Time Monitoring of Drug Release. ACS Nano, 2014, 8, 5939-5952.	14.6	102
132	Multifunctional Bismuth Ferrite Nanocatalysts with Optical and Magnetic Functions for Ultrasound-Enhanced Tumor Theranostics. ACS Nano, 2020, 14, 7245-7258.	14.6	101
133	Clicked Isoreticular Metal–Organic Frameworks and Their High Performance in the Selective Capture and Separation of Large Organic Molecules. Angewandte Chemie - International Edition, 2015, 54, 12748-12752.	13.8	99
134	Linkage Engineering by Harnessing Supramolecular Interactions to Fabricate 2D Hydrazone-Linked Covalent Organic Framework Platforms toward Advanced Catalysis. Journal of the American Chemical Society, 2020, 142, 18138-18149.	13.7	99
135	Pyrenecyclodextrinâ€Decorated Singleâ€Walled Carbon Nanotube Fieldâ€Effect Transistors as Chemical Sensors. Advanced Materials, 2008, 20, 1910-1915.	21.0	98
136	Pillararene/Calixarene-based systems for battery and supercapacitor applications. EScience, 2021, 1, 28-43.	41.6	97
137	Enhanced photocatalytic water oxidation by hierarchical 2D-Bi2MoO6@2D-MXene Schottky junction nanohybrid. Chemical Engineering Journal, 2021, 403, 126328.	12.7	94
138	Luminescent Color Conversion on Cyanostilbeneâ€Functionalized Quantum Dots via Inâ€situ Photoâ€Tuning. Advanced Materials, 2012, 24, 4020-4024.	21.0	93
139	Cyclometalated Iridium(III)-Complex-Based Micelles for Glutathione-Responsive Targeted Chemotherapy and Photodynamic Therapy. ACS Applied Materials & amp; Interfaces, 2017, 9, 27553-27562.	8.0	93
140	Recent advances in biocompatible nanocarriers for delivery of chemotherapeutic cargoes towards cancer therapy. Organic and Biomolecular Chemistry, 2014, 12, 4776.	2.8	92
141	Trace Carbon Dioxide Capture by Metal–Organic Frameworks. ACS Sustainable Chemistry and Engineering, 2019, 7, 82-93.	6.7	92
142	Two-dimensional covalent–organic frameworks for ultrahigh iodine capture. Journal of Materials Chemistry A, 2020, 8, 9523-9527.	10.3	92
143	Acid-Responsive Polymeric Doxorubicin Prodrug Nanoparticles Encapsulating a Near-Infrared Dye for Combined Photothermal-Chemotherapy. Chemistry of Materials, 2016, 28, 7039-7050.	6.7	90
144	An aza-BODIPY based near-infrared fluorescent probe for sensitive discrimination of cysteine/homocysteine and glutathione in living cells. Chemical Communications, 2017, 53, 5220-5223.	4.1	90

#	Article	IF	CITATIONS
145	Mechanical Bond-Induced Radical Stabilization. Journal of the American Chemical Society, 2013, 135, 456-467.	13.7	89
146	Recent Advances in Covalent Organic Framework-Based Nanosystems for Bioimaging and Therapeutic Applications. , 2020, 2, 1074-1092.		89
147	Rigidâ€Strutâ€Containing Crown Ethers and [2]Catenanes for Incorporation into Metal–Organic Frameworks. Chemistry - A European Journal, 2009, 15, 13356-13380.	3.3	88
148	Self-assembled organic nanomedicine enables ultrastable photo-to-heat converting theranostics in the second near-infrared biowindow. Nature Communications, 2021, 12, 218.	12.8	88
149	Vanadium-based polyoxometalate as new material for sodium-ion battery anodes. Journal of Power Sources, 2015, 288, 270-277.	7.8	87
150	Click chemistry as a versatile reaction for construction and modification of metal-organic frameworks. Coordination Chemistry Reviews, 2019, 380, 484-518.	18.8	86
151	Thermo-responsive fluorescent vesicles assembled by fluorescein-functionalized pillar[5]arene. RSC Advances, 2013, 3, 368-371.	3.6	85
152	Host–guest complexation driven dynamic supramolecular self-assembly. Organic and Biomolecular Chemistry, 2013, 11, 2070.	2.8	84
153	Self-Assembled Hybrid Nanostructures: Versatile Multifunctional Nanoplatforms for Cancer Diagnosis and Therapy. Chemistry of Materials, 2018, 30, 25-53.	6.7	83
154	Crystal Multiâ€Conformational Control Through Deformable Carbonâ€Sulfur Bond for Singletâ€Triplet Emissive Tuning. Angewandte Chemie - International Edition, 2019, 58, 4328-4333.	13.8	82
155	Strain-Engineering of Bi <sub>12</sub> O <sub>17</sub> Br <sub>2</sub> Nanotubes for Boosting Photocatalytic CO <sub>2</sub> Reduction. , 2020, 2, 1025-1032.		82
156	Nanozymes: Versatile Platforms for Cancer Diagnosis and Therapy. Nano-Micro Letters, 2022, 14, 95.	27.0	82
157	Fabrication of Ruthenium Nanoparticles in Porous Organic Polymers: Towards Advanced Heterogeneous Catalytic Nanoreactors. Chemistry - A European Journal, 2015, 21, 19016-19027.	3.3	81
158	Occurrence of Chiral Nanostructures Induced by Multiple Hydrogen Bonds. Journal of the American Chemical Society, 2019, 141, 9946-9954.	13.7	81
159	Hierarchical NiO@Nâ€Đoped Carbon Microspheres with Ultrathin Nanosheet Subunits as Excellent Photocatalysts for Hydrogen Evolution. Small, 2019, 15, e1901024.	10.0	81
160	Synergistic Effect of Mesoporous Co <sub>3</sub> O <sub>4</sub> Nanowires Confined by N-Doped Graphene Aerogel for Enhanced Lithium Storage. Small, 2016, 12, 3849-3860.	10.0	80
161	Chiral covalent organic frameworks for asymmetric catalysis and chiral separation. Science China Chemistry, 2017, 60, 1015-1022.	8.2	79
162	Surfactant–Thermal Method to Synthesize a Novel Twoâ€Dimensional Oxochalcogenide. Chemistry - an Asian Journal, 2014, 9, 131-134.	3.3	78

#	Article	IF	CITATIONS
163	Construction of Covalentâ€Organic Frameworks (COFs) from Amorphous Covalent Organic Polymers via Linkage Replacement. Angewandte Chemie - International Edition, 2019, 58, 17679-17683.	13.8	78
164	Structure Tuning of Polymeric Carbon Nitride for Solar Energy Conversion: From Nano to Molecular Scale. CheM, 2019, 5, 2775-2813.	11.7	78
165	State-of-the-art iron-based nanozymes for biocatalytic tumor therapy. Nanoscale Horizons, 2020, 5, 202-217.	8.0	78
166	NIR-triggered drug release from switchable rotaxane-functionalized silica-covered Au nanorods. Chemical Communications, 2014, 50, 9745.	4.1	77
167	Light-Responsive Prodrug-Based Supramolecular Nanosystems for Site-Specific Combination Therapy of Cancer. Chemistry of Materials, 2019, 31, 3349-3358.	6.7	77
168	A Novel Strategy for the Construction of Covalent Organic Frameworks from Nonporous Covalent Organic Polymers. Angewandte Chemie - International Edition, 2019, 58, 4906-4910.	13.8	76
169	Structure–performance correlation guided applications of covalent organic frameworks. Materials Today, 2022, 53, 106-133.	14.2	76
170	Fourâ€inâ€One Stimulusâ€Responsive Longâ€Lived Luminescent Systems Based on Pyreneâ€Doped Amorphous Polymers. Angewandte Chemie - International Edition, 2022, 61, .	13.8	76
171	Incorporation of thio-pseudoisocytosine into triplex-forming peptide nucleic acids for enhanced recognition of RNA duplexes. Nucleic Acids Research, 2014, 42, 4008-4018.	14.5	75
172	Recent advances in multifunctional silica-based hybrid nanocarriers for bioimaging and cancer therapy. Nanoscale, 2016, 8, 12510-12519.	5.6	75
173	Metal–Organic Framework Derived Multicomponent Nanoagent as a Reactive Oxygen Species Amplifier for Enhanced Photodynamic Therapy. ACS Nano, 2020, 14, 13500-13511.	14.6	75
174	Helicity Inversion of Supramolecular Hydrogels Induced by Achiral Substituents. ACS Nano, 2017, 11, 11880-11889.	14.6	74
175	Supramolecular nanoparticle carriers self-assembled from cyclodextrin- and adamantane-functionalized polyacrylates for tumor-targeted drug delivery. Journal of Materials Chemistry B, 2014, 2, 1879.	5.8	73
176	[4 + 2] Cycloaddition Reaction To Approach Diazatwistpentacenes: Synthesis, Structures, Physical Properties, and Self-assembly. Journal of Organic Chemistry, 2014, 79, 4438-4445.	3.2	72
177	Polymeric Prodrug Grafted Hollow Mesoporous Silica Nanoparticles Encapsulating Near-Infrared Absorbing Dye for Potent Combined Photothermal-Chemotherapy. ACS Applied Materials & Interfaces, 2016, 8, 6869-6879.	8.0	70
178	Multifunctional metal-organic framework-based nanoreactor for starvation/oxidation improved indoleamine 2,3-dioxygenase-blockade tumor immunotherapy. Nature Communications, 2022, 13, 2688.	12.8	70
179	Functional Silica Nanoparticles for Redoxâ€Triggered Drug/ssDNA Coâ€delivery. Advanced Healthcare Materials, 2012, 1, 690-697.	7.6	69
180	Carbon Quantum Dot Implanted Graphite Carbon Nitride Nanotubes: Excellent Charge Separation and Enhanced Photocatalytic Hydrogen Evolution. Angewandte Chemie, 2018, 130, 5867-5873.	2.0	69

#	Article	IF	CITATIONS
181	Ultrathin ZnIn <sub>2</sub> S <sub>4</sub> Nanosheets Anchored on Ti <sub>3</sub> C <sub>2</sub> T <sub><i>X</i></sub> MXene for Photocatalytic H <sub>2</sub> Evolution. Angewandte Chemie, 2020, 132, 11383-11388.	2.0	69
182	Industrializing metal–organic frameworks: Scalable synthetic means and their transformation into functional materials. Materials Today, 2021, 47, 170-186.	14.2	69
183	Light-Controllable Cucurbit[7]uril-Based Molecular Shuttle. Journal of Organic Chemistry, 2012, 77, 10168-10175.	3.2	68
184	Chirality Control for in Situ Preparation of Gold Nanoparticle Superstructures Directed by a Coordinatable Organogelator. Journal of the American Chemical Society, 2013, 135, 9174-9180.	13.7	68
185	A ratiometric fluorescent molecular probe with enhanced two-photon response upon Zn <sup>2+</sup> binding for in vitro and in vivo bioimaging. Chemical Science, 2014, 5, 3469-3474.	7.4	68
186	Molecular Phosphorescence in Polymer Matrix with Reversible Sensitivity. ACS Applied Materials & Interfaces, 2020, 12, 20765-20774.	8.0	68
187	Spectrophotometric Study of Inclusion Complexation of Aliphatic Alcohols byβ-Cyclodextrins with Azobenzene Tether. Journal of Physical Chemistry B, 2004, 108, 8836-8843.	2.6	67
188	Synthesis of Microporous Nitrogenâ€Rich Covalentâ€Organic Framework and Its Application in CO <sub>2</sub> Capture. Chinese Journal of Chemistry, 2015, 33, 90-94.	4.9	67
189	Single-Site Palladium(II) Catalyst for Oxidative Heck Reaction: Catalytic Performance and Kinetic Investigations. ACS Catalysis, 2015, 5, 3752-3759.	11.2	66
190	Redox and pH Dual Responsive Polymer Based Nanoparticles for In Vivo Drug Delivery. Small, 2017, 13, 1602379.	10.0	66
191	Tailoring TiO <sub>2</sub> Nanotubeâ€Interlaced Graphite Carbon Nitride Nanosheets for Improving Visibleâ€Lightâ€Driven Photocatalytic Performance. Advanced Science, 2018, 5, 1700844.	11.2	66
192	Accurate synergy effect of Ni–Sn dual active sites enhances electrocatalytic oxidation of urea for hydrogen evolution in alkaline medium. Journal of Materials Chemistry A, 2020, 8, 14680-14689.	10.3	66
193	Supramolecular Polypseudorotaxane with Conjugated Polyazomethine Prepared Directly from Two Inclusion Complexes of β-Cyclodextrin with Tolidine and Phthaldehyde. Macromolecules, 2004, 37, 6362-6369.	4.8	65
194	Nearâ€Infrared Lightâ€Absorptive Stealth Liposomes for Localized Photothermal Ablation of Tumors Combined with Chemotherapy. Advanced Functional Materials, 2015, 25, 5602-5610.	14.9	65
195	Unexpected right-handed helical nanostructures co-assembled from <scp>l</scp> -phenylalanine derivatives and achiral bipyridines. Chemical Science, 2017, 8, 1769-1775.	7.4	65
196	Molecular Engineering for Metalâ€Free Amorphous Materials with Roomâ€Temperature Phosphorescence. Angewandte Chemie, 2020, 132, 11302-11312.	2.0	65
197	Photosensitizer anchored gold nanorods for targeted combinational photothermal and photodynamic therapy. Chemical Communications, 2016, 52, 8854-8857.	4.1	64
198	Responsive mesoporous silica nanoparticles for sensing of hydrogen peroxide and simultaneous treatment toward heart failure. Nanoscale, 2017, 9, 2253-2261.	5.6	64

#	Article	IF	CITATIONS
199	Construction and DNA Condensation of Cyclodextrin-Based Polypseudorotaxanes with Anthryl Grafts. Journal of the American Chemical Society, 2007, 129, 10656-10657.	13.7	63
200	Real time monitoring of aminothiol level in blood using a near-infrared dye assisted deep tissue fluorescence and photoacoustic bimodal imaging. Chemical Science, 2016, 7, 4110-4116.	7.4	63
201	Superstructure Formation and Topological Evolution Achieved by Self-Organization of a Highly Adaptive Dynamer. ACS Nano, 2016, 10, 2716-2727.	14.6	63
202	Selective Coassembly of Aromatic Amino Acids to Fabricate Hydrogels with Light Irradiationâ€Induced Emission for Fluorescent Imprint. Advanced Materials, 2018, 30, 1705633.	21.0	63
203	A H2O2-activatable nanoprobe for diagnosing interstitial cystitis and liver ischemia-reperfusion injury via multispectral optoacoustic tomography and NIR-II fluorescent imaging. Nature Communications, 2021, 12, 6870.	12.8	63
204	CuO Nanoparticles Deposited on Nanoporous Polymers: A Recyclable Heterogeneous Nanocatalyst for Ullmann Coupling of Aryl Halides with Amines in Water. Scientific Reports, 2015, 5, 8294.	3.3	62
205	Enhanced performance in gas adsorption and Li ion batteries by docking Li <sup>+</sup> in a crown ether-based metal–organic framework. Chemical Communications, 2016, 52, 3003-3006.	4.1	62
206	"Click―extended nitrogen-rich metal–organic frameworks and their high performance in CO2-selective capture. Chemical Communications, 2014, 50, 4683.	4.1	61
207	Solution-processed black phosphorus/PCBM hybrid heterojunctions for solar cells. Journal of Materials Chemistry A, 2017, 5, 8280-8286.	10.3	60
208	Preparation of Ultrathin Twoâ€Dimensional Ti <sub><i>x</i></sub> Ta <sub>1â^`<i>x</i></sub> S <sub><i>y</i></sub> O <sub><i>z</i></sub> Nanosheets as Highly Efficient Photothermal Agents. Angewandte Chemie - International Edition, 2017, 56, 7842-7846.	13.8	59
209	Supramolecular Vesicles for Stimulusâ€Responsive DrugÂDelivery. Small Methods, 2018, 2, 1700364.	8.6	59
210	MTH1 inhibitor amplifies the lethality of reactive oxygen species to tumor in photodynamic therapy. Science Advances, 2020, 6, eaaz0575.	10.3	59
211	Protein-Based Nanomedicine for Therapeutic Benefits of Cancer. ACS Nano, 2021, 15, 8001-8038.	14.6	59
212	Oxygen vacancy mediated bismuth stannate ultra-small nanoparticle towards photocatalytic CO2-to-CO conversion. Applied Catalysis B: Environmental, 2020, 276, 119156.	20.2	59
213	Photoswitchable Supramolecular Catalysis by Interparticle Host–Guest Competitive Binding. Chemistry - A European Journal, 2012, 18, 13979-13983.	3.3	58
214	Emerging contrast agents for multispectral optoacoustic imaging and their biomedical applications. Chemical Society Reviews, 2021, 50, 7924-7940.	38.1	58
215	A Tunable Photosensor. Journal of the American Chemical Society, 2008, 130, 16996-17003.	13.7	57
216	Photo-triggered transformation from vesicles to branched nanotubes fabricated by a cholesterol-appended cyanostilbene. Chemical Communications, 2015, 51, 9309-9312.	4.1	57

#	Article	IF	CITATIONS
217	Polymeric nanocarriers incorporating near-infrared absorbing agents for potent photothermal therapy of cancer. Polymer Journal, 2016, 48, 589-603.	2.7	57
218	Fast learable Nanocarriers Conducting Chemo/Photothermal Combination Therapy to Inhibit Recurrence of Malignant Tumors. Small, 2017, 13, 1700963.	10.0	57
219	Selfâ€5orting Doubleâ€Network Hydrogels with Tunable Supramolecular Handedness and Mechanical Properties. Angewandte Chemie - International Edition, 2019, 58, 9366-9372.	13.8	57
220	Self-Assembled Oxaliplatin(IV) Prodrug–Porphyrin Conjugate for Combinational Photodynamic Therapy and Chemotherapy. ACS Applied Materials & Interfaces, 2019, 11, 16391-16401.	8.0	56
221	Spacer Intercalated Disassembly and Photodynamic Activity of Zinc Phthalocyanine Inside Nanochannels of Mesoporous Silica Nanoparticles. ACS Applied Materials & Interfaces, 2013, 5, 12860-12868.	8.0	55
222	Clearable Black Phosphorus Nanoconjugate for Targeted Cancer Phototheranostics. ACS Applied Materials & Interfaces, 2020, 12, 18342-18351.	8.0	55
223	Single-atom engineering of metal-organic frameworks toward healthcare. CheM, 2021, 7, 2635-2671.	11.7	55
224	Redox-Responsive Mesoporous Silica Nanoparticles: A Physiologically Sensitive Codelivery Vehicle for siRNA and Doxorubicin. Antioxidants and Redox Signaling, 2014, 21, 707-722.	5.4	53
225	Understanding Pathway Complexity of Organic Micro/Nanofiber Growth in Hydrogen-Bonded Coassembly of Aromatic Amino Acids. ACS Nano, 2017, 11, 4206-4216.	14.6	53
226	Synergistically enhanced charge separation in BiFeO3/Sn:TiO2 nanorod photoanode via bulk and surface dual modifications. Nano Energy, 2019, 59, 33-40.	16.0	53
227	Assembly behavior of inclusion complexes of β-cyclodextrin with 4-hydroxyazobenzene and 4-aminoazobenzene. Organic and Biomolecular Chemistry, 2005, 3, 584-591.	2.8	52
228	Sizeâ€Transformable Nanostructures: From Design to Biomedical Applications. Advanced Materials, 2020, 32, e2003752.	21.0	52
229	Reconstruction of Covalent Organic Frameworks by Dynamic Equilibrium. Chemistry - A European Journal, 2015, 21, 16818-16822.	3.3	51
230	Three-Photon-Excited Luminescence from Unsymmetrical Cyanostilbene Aggregates: Morphology Tuning and Targeted Bioimaging. ACS Nano, 2015, 9, 4796-4805.	14.6	51
231	Cu <sub>2–<i>x</i></sub> S Nanocrystals Cross-Linked with Chlorin e6-Functionalized Polyethylenimine for Synergistic Photodynamic and Photothermal Therapy of Cancer. ACS Applied Materials & Interfaces, 2018, 10, 16344-16351.	8.0	51
232	Recent advancements in 2D nanomaterials for cancer therapy. Science China Chemistry, 2018, 61, 1214-1226.	8.2	51
233	The Art of Integrated Functionalization: Super Stable Black Phosphorus Achieved through Metalâ€Organic Framework Coating. Advanced Functional Materials, 2020, 30, 2002232.	14.9	51
234	The Structures and Thermodynamics of Complexes between Water-Soluble Calix[4]arenes and Dipyridinium lons. European Journal of Organic Chemistry, 2005, 2005, 162-170.	2.4	50

#	Article	IF	CITATIONS
235	Towards rational design of core–shell catalytic nanoreactor with high performance catalytic hydrogenation of levulinic acid. Catalysis Science and Technology, 2016, 6, 5102-5115.	4.1	50
236	Environmentâ€Adaptive Coassembly/Selfâ€Sorting and Stimulusâ€Responsiveness Transfer Based on Cholesterol Building Blocks. Advanced Science, 2018, 5, 1700552.	11.2	50
237	Combined Photodynamic and Photothermal Therapy Using Cross-Linked Polyphosphazene Nanospheres Decorated with Gold Nanoparticles. ACS Applied Nano Materials, 2018, 1, 3663-3672.	5.0	50
238	Diverse Role of Solvents in Controlling Supramolecular Chirality. Chemistry - A European Journal, 2019, 25, 7426-7437.	3.3	50
239	Incorporating Photochromic Triphenylamine into a Zirconium–Organic Framework for Highly Effective Photocatalytic Aerobic Oxidation of Sulfides. ACS Applied Materials & Interfaces, 2021, 13, 20137-20144.	8.0	50
240	Imaging-Guided Drug Release from Glutathione-Responsive Supramolecular Porphysome Nanovesicles. ACS Applied Materials & Interfaces, 2015, 7, 17371-17380.	8.0	49
241	VOPO <sub>4</sub> ·2H <sub>2</sub> O encapsulated in graphene oxide as a heterogeneous catalyst for selective hydroxylation of benzene to phenol. Green Chemistry, 2016, 18, 397-401.	9.0	49
242	Excitationâ€Dependent Longâ€Life Luminescent Polymeric Systems under Ambient Conditions. Angewandte Chemie, 2020, 132, 10053-10057.	2.0	49
243	A Transferrin-Conjugated Hollow Nanoplatform for Redox-Controlled and Targeted Chemotherapy of Tumor with Reduced Inflammatory Reactions. Theranostics, 2018, 8, 518-532.	10.0	48
244	Ultrafast Low-Temperature Photothermal Therapy Activates Autophagy and Recovers Immunity for Efficient Antitumor Treatment. ACS Applied Materials & amp; Interfaces, 2020, 12, 4265-4275.	8.0	48
245	Silica–Polymer Hybrid with Selfâ€Assembled PEG Corona Excreted Rapidly via a Hepatobiliary Route. Advanced Functional Materials, 2016, 26, 3036-3047.	14.9	47
246	Precise Chemodynamic Therapy of Cancer by Trifunctional Bacterium-Based Nanozymes. ACS Nano, 2021, 15, 19321-19333.	14.6	47
247	Working Mechanism for a Redox Switchable Molecular Machine Based on Cyclodextrin: A Free Energy Profile Approach. Journal of Physical Chemistry B, 2010, 114, 6561-6566.	2.6	46
248	Theranostic Prodrug Vesicles for Imaging Guided Codelivery of Camptothecin and siRNA in Synergetic Cancer Therapy. ACS Applied Materials & amp; Interfaces, 2017, 9, 23536-23543.	8.0	46
249	Glutathioneâ€Depleting Organic Metal Adjuvants for Effective NIRâ€II Photothermal Immunotherapy. Advanced Materials, 2022, 34, e2201706.	21.0	46
250	Efficient alkene hydrogenation over a magnetically recoverable and recyclable Fe3O4@GO nanocatalyst using hydrazine hydrate as the hydrogen source. Chemical Communications, 2014, 50, 12095-12097.	4.1	45
251	Intracellular Delivery of Antisense Peptide Nucleic Acid by Fluorescent Mesoporous Silica Nanoparticles. Bioconjugate Chemistry, 2014, 25, 1412-1420.	3.6	45
252	Narrow bandgap thienothiadiazole-based conjugated porous polymers: from facile direct arylation polymerization to tunable porosities and optoelectronic properties. Polymer Chemistry, 2016, 7, 6413-6421.	3.9	45

#	Article	IF	CITATIONS
253	Waterâ€Bindingâ€Mediated Gelation/Crystallization and Thermosensitive Superchirality. Angewandte Chemie - International Edition, 2018, 57, 7774-7779.	13.8	45
254	Selective Thrombosis of Tumor for Enhanced Hypoxiaâ€Activated Prodrug Therapy. Advanced Materials, 2021, 33, e2104504.	21.0	45
255	Photoâ€Induced Dynamic Room Temperature Phosphorescence Based on Triphenyl Phosphonium Containing Polymers. Advanced Functional Materials, 2022, 32, .	14.9	45
256	Functionally Rigid and Degenerate Molecular Shuttles. Chemistry - A European Journal, 2009, 15, 1115-1122.	3.3	44
257	Surfactant-Thermal Syntheses, Structures, and Magnetic Properties of Mn–Ge–Sulfides/Selenides. Inorganic Chemistry, 2014, 53, 10248-10256.	4.0	44
258	Nanodot-Directed Formation of Plasmonic-Fluorescent Nanohybrids toward Dual Optical Detection of Glucose and Cholesterol via Hydrogen Peroxide Sensing. ACS Applied Materials & Interfaces, 2019, 11, 27233-27242.	8.0	44
259	In Situ Nanozymeâ€Amplified NIRâ€II Phototheranostics for Tumorâ€Specific Imaging and Therapy. Advanced Functional Materials, 2021, 31, 2103765.	14.9	44
260	Microporous polymelamine network for highly selective CO2 adsorption. Polymer, 2013, 54, 596-600.	3.8	43
261	Photoresponsive real time monitoring silicon quantum dots for regulated delivery of anticancer drugs. Journal of Materials Chemistry B, 2016, 4, 521-528.	5.8	43
262	"Greener―and modular synthesis of triazine-based conjugated porous polymers <i>via</i> direct arylation polymerization: structure–function relationship and photocatalytic application. Polymer Chemistry, 2018, 9, 1972-1982.	3.9	43
263	Solventâ€Controlled Assembly of Aromatic Clutamic Dendrimers for Efficient Luminescent Color Conversion. Advanced Functional Materials, 2018, 28, 1802859.	14.9	43
264	Spatial engineering of a Co(OH) <sub>x</sub> encapsulated p-Cu <sub>2</sub> S/n-BiVO <sub>4</sub> photoanode: simultaneously promoting charge separation and surface reaction kinetics in solar water splitting. Journal of Materials Chemistry A, 2019, 7, 6747-6752.	10.3	43
265	Photoinduced Radical Emission in a Coassembly System. Angewandte Chemie - International Edition, 2021, 60, 23842-23848.	13.8	43
266	A water-soluble β-cyclodextrin derivative possessing a fullerene tether as an efficient photodriven DNA-cleavage reagent. Tetrahedron Letters, 2005, 46, 2507-2511.	1.4	42
267	Ruthenium bipyridyl tethered porous organosilica: a versatile, durable and reusable heterogeneous photocatalyst. Chemical Communications, 2015, 51, 10746-10749.	4.1	42
268	Anticancer Effect of α-Tocopheryl Succinate Delivered by Mitochondria-Targeted Mesoporous Silica Nanoparticles. ACS Applied Materials & Interfaces, 2016, 8, 34261-34269.	8.0	42
269	Refined Sulfur Nanoparticles Immobilized in Metal–Organic Polyhedron as Stable Cathodes for Li–S Battery. ACS Applied Materials & Interfaces, 2016, 8, 14328-14333.	8.0	42
270	Proteinâ€Based Artificial Nanosystems in Cancer Therapy. Small, 2020, 16, 1907256.	10.0	42

#	Article	IF	CITATIONS
271	Dual Gateâ€Controlled Therapeutics for Overcoming Bacteriumâ€Induced Drug Resistance and Potentiating Cancer Immunotherapy. Angewandte Chemie - International Edition, 2021, 60, 14013-14021.	13.8	42
272	Cu-Grafted Functionalized Mesoporous SBA-15: A Novel Heterogeneous Catalyst for Facile One-Pot Three-Component C–S Cross-Coupling Reaction of Aryl Halides in Water. Organic Process Research and Development, 2014, 18, 257-265.	2.7	41
273	Waterâ€Soluble Pillarareneâ€Functionalized Graphene Oxide for Inâ€Vitro Raman and Fluorescence Dualâ€Mode Imaging. ChemPlusChem, 2014, 79, 462-469.	2.8	41
274	Rationally encapsulated gold nanorods improving both linear and nonlinear photoacoustic imaging contrast in vivo. Nanoscale, 2017, 9, 79-86.	5.6	41
275	Programmable Multicomponent Selfâ€Assembly Based on Aromatic Amino Acids. Advanced Materials, 2018, 30, e1805175.	21.0	41
276	[enH][Cu <sub>2</sub> AgSnS <sub>4</sub> ]: a quaternary layered sulfide based on Cu–Ag–Sn–S composition. CrystEngComm, 2014, 16, 5989-5992.	2.6	40
277	Photocontrolled Nuclear-Targeted Drug Delivery by Single Component Photoresponsive Fluorescent Organic Nanoparticles of Acridin-9-Methanol. Bioconjugate Chemistry, 2013, 24, 1828-1839.	3.6	38
278	Synthesis, physical properties and OLED performance of azatetracenes. Dyes and Pigments, 2015, 112, 93-98.	3.7	38
279	Tuning Synergistic Effect of Au–Pd Bimetallic Nanocatalyst for Aerobic Oxidative Carbonylation of Amines. Chemistry of Materials, 2017, 29, 3671-3677.	6.7	38
280	Redox-Responsive Polymeric Nanocomplex for Delivery of Cytotoxic Protein and Chemotherapeutics. ACS Applied Materials & Interfaces, 2019, 11, 31638-31648.	8.0	38
281	Molecular Expansion for Constructing Porous Organic Polymers with High Surface Areas and Wellâ€Đefined Nanopores. Angewandte Chemie - International Edition, 2020, 59, 19487-19493.	13.8	38
282	High iodine uptake in two-dimensional covalent organic frameworks. Chemical Communications, 2021, 57, 5558-5561.	4.1	38
283	Effective Photocatalytic Initiation of Reactive Oxygen Species by a Photoactive Covalent Organic Framework for Oxidation Reactions. , 2022, 4, 1160-1167.		38
284	On-Demand Generation of Peroxynitrite from an Integrated Two-Dimensional System for Enhanced Tumor Therapy. ACS Nano, 2022, 16, 8939-8953.	14.6	38
285	Bis(pseudopolyrotaxane)s Possessing Copper(II) Ions Formed by Different Polymer Chains and Bis(l²-cyclodextrin)s Bridged with a 2,2'-Bipyridine-4,4'-Dicarboxy Tether. Macromolecules, 2002, 35, 9934-9938.	4.8	37
286	Degenerate [2]rotaxanes with electrostatic barriers. Organic and Biomolecular Chemistry, 2011, 9, 2240.	2.8	37
287	Highâ€Performance Titanosilicate Catalyst Obtained through Combination of Liquidâ€Phase and Solidâ€Phase Transformation Mechanisms. ChemCatChem, 2014, 6, 2719-2726.	3.7	37
288	Recent developments in porous materials for H2 and CH4 storage. Tetrahedron Letters, 2016, 57, 4873-4881.	1.4	37

#	Article	IF	CITATIONS
289	Catalytic asymmetric acetalization of carboxylic acids for access to chiral phthalidyl ester prodrugs. Nature Communications, 2019, 10, 1675.	12.8	37
290	Regulating the reactivity of black phosphorus via protective chemistry. Science Advances, 2020, 6, .	10.3	37
291	Pillararene-based self-assemblies for electrochemical biosensors. Biosensors and Bioelectronics, 2021, 181, 113164.	10.1	37
292	Photoinduced Charge Transfer within Polyaniline-Encapsulated Quantum Dots Decorated on Graphene. ACS Applied Materials & Interfaces, 2013, 5, 8105-8110.	8.0	36
293	Responsive Prodrug Self-Assembled Vesicles for Targeted Chemotherapy in Combination with Intracellular Imaging. ACS Applied Materials & Interfaces, 2016, 8, 24319-24324.	8.0	36
294	Robust Amphiphobic Few‣ayer Black Phosphorus Nanosheet with Improved Stability. Advanced Science, 2019, 6, 1901991.	11.2	36
295	Amorphous Ionic Polymers with Colorâ€īunable Ultralong Organic Phosphorescence. Angewandte Chemie, 2019, 131, 18952-18958.	2.0	36
296	Long-Lived Room Temperature Phosphorescence Crystals with Green Light Excitation. ACS Applied Materials & Interfaces, 2022, 14, 15706-15715.	8.0	36
297	Supramolecular Assembly of Gold Nanoparticles Mediated by Polypseudorotaxane with Thiolated?-Cyclodextrin. Macromolecular Rapid Communications, 2005, 26, 401-406.	3.9	35
298	Sequential self-assembly for construction of Pt(ii)-bridged [3]rotaxanes on gold nanoparticles. Chemical Communications, 2012, 48, 4290.	4.1	35
299	Fabrication of novel hybrid nanoflowers from boron nitride nanosheets and metal–organic frameworks: a solid acid catalyst with enhanced catalytic performance. Journal of Materials Chemistry A, 2014, 2, 18731-18735.	10.3	35
300	Co(II)-tricarboxylate metal–organic frameworks constructed from solvent-directed assembly for CO2 adsorption. Microporous and Mesoporous Materials, 2013, 176, 194-198.	4.4	34
301	Macroscopic Architecture of Charge Transfer-Induced Molecular Recognition from Electron-Rich Polymer Interpenetrated Porous Frameworks. ACS Applied Materials & Interfaces, 2015, 7, 5056-5060.	8.0	34
302	A dual responsive "turn-on―fluorophore for orthogonal selective sensing of biological thiols and hydrogen peroxide. Journal of Materials Chemistry C, 2016, 4, 2761-2774.	5.5	34
303	Switching between Phosphorescence and Fluorescence Controlled by Chiral Selfâ€Assembly. Advanced Science, 2017, 4, 1700021.	11.2	34
304	Liquid-Crystalline Hydroxyapatite/Polymer Nanorod Hybrids: Potential Bioplatform for Photodynamic Therapy and Cellular Scaffolds. ACS Applied Materials & Interfaces, 2019, 11, 17759-17765.	8.0	34
305	Genetically modified bacteria for targeted phototherapy of tumor. Biomaterials, 2021, 272, 120809.	11.4	34
306	A urea decorated (3,24)-connected rht-type metal–organic framework exhibiting high gas uptake capability and catalytic activity. CrystEngComm, 2015, 17, 4632-4636.	2.6	33

#	Article	IF	CITATIONS
307	Organic–inorganic nanohybrids for fluorescence, photoacoustic and Raman bioimaging. Science Bulletin, 2015, 60, 665-678.	9.0	33
308	Light and cucurbit[7]uril complexation dual-responsiveness of a cyanostilbene-based self-assembled system. Nanoscale, 2016, 8, 1892-1896.	5.6	33
309	Metal-ligated pillararene materials: From chemosensors to multidimensional self-assembled architectures. Coordination Chemistry Reviews, 2020, 420, 213425.	18.8	33
310	Bundle-Shaped Cyclodextrinâ^'Tb Nano-Supramolecular Assembly Mediated by C60:Â Intramolecular Energy Transfer. Nano Letters, 2006, 6, 2196-2200.	9.1	32
311	Morphologyâ€Tuned Exceptional Catalytic Activity of Porousâ€Polymerâ€Supported Mn <sub>3</sub> O <sub>4</sub> in Aerobic sp <sup>3</sup> CH Bond Oxidation of Aromatic Hydrocarbons and Alcohols. ChemCatChem, 2014, 6, 3518-3529.	3.7	32
312	Urea–pyridine bridged periodic mesoporous organosilica: An efficient hydrogen-bond donating heterogeneous organocatalyst for Henry reaction. Journal of Catalysis, 2015, 330, 129-134.	6.2	32
313	Incorporating a guanidine-modified cytosine base into triplex-forming PNAs for the recognition of a C-G pyrimidine–purine inversion site of an RNA duplex. Nucleic Acids Research, 2016, 44, gkw778.	14.5	32
314	Ruthenium-Catalyzed Oxidative Homocoupling of Arylboronic Acids in Water: Ligand Tuned Reactivity and Mechanistic Study. Inorganic Chemistry, 2016, 55, 6332-6343.	4.0	32
315	Independent of EPR Effect: A Smart Delivery Nanosystem for Tracking and Treatment of Nonvascularized Intraâ€Abdominal Metastases. Advanced Functional Materials, 2018, 28, 1806162.	14.9	32
316	Facile preparation of antibacterial MOFâ€fabric systems for functional protective wearables. SmartMat, 2021, 2, 567-578.	10.7	32
317	Cell-Specific Metabolic Reprogramming of Tumors for Bioactivatable Ferroptosis Therapy. ACS Nano, 2022, 16, 3965-3984.	14.6	32
318	Binding Ability and Assembly Behavior ofβ-Cyclodextrin Complexes with 2,2â€~-Dipyridine and 4,4â€~-Dipyridine. Journal of Organic Chemistry, 2004, 69, 3383-3390.	3.2	31
319	Synthesis of Bridged and Metallobridged Bis(β-cyclodextrin)s Containing Fluorescent Oxamidobisbenzoyl Linkers and Their Selective Binding towards Bile Salts. Chemistry - A European Journal, 2006, 12, 3858-3868.	3.3	31
320	Surfactant-thermal method to prepare two novel two-dimensional Mn–Sb–S compounds for photocatalytic applications. Journal of Solid State Chemistry, 2014, 220, 118-123.	2.9	31
321	Pyridiniumâ€Fused Pyridinone: A Novel "Turnâ€on―Fluorescent Chemodosimeter for Cyanide. Chemistry - an Asian Journal, 2014, 9, 121-125.	3.3	31
322	Host–Guest Interactionâ€Mediated Construction of Hydrogels and Nanovesicles for Drug Delivery. Small, 2015, 11, 5901-5906.	10.0	31
323	Remarkable In Vivo Nonlinear Photoacoustic Imaging Based on Near-Infrared Organic Dyes. Small, 2016, 12, 5239-5244.	10.0	31
324	Tailoring luminescence color conversion via affinitive co-assembly of glutamates appended with pyrene and naphthalene dicarboximide units. Chemical Communications, 2016, 52, 1246-1249.	4.1	31

#	Article	IF	CITATIONS
325	A highly porous metal–organic framework for large organic molecule capture and chromatographic separation. Chemical Communications, 2017, 53, 3434-3437.	4.1	31
326	Tumorâ€Microenvironmentâ€Activated In Situ Selfâ€Assembly of Sequentially Responsive Biopolymer for Targeted Photodynamic Therapy. Advanced Functional Materials, 2020, 30, 2000229.	14.9	31
327	Fluorescent Imprintable Hydrogels via Organic/Inorganic Supramolecular Coassembly. ACS Applied Materials & Interfaces, 2020, 12, 15491-15499.	8.0	31
328	Spectrophotometric Study of Fluorescence Sensing and Selective Binding of Biochemical Substrates by 2,2â€~-Bridged Bis(β-cyclodextrin) and Its Water-Soluble Fullerene Conjugate. Journal of Physical Chemistry B, 2005, 109, 23739-23744.	2.6	30
329	"Turn-on―fluorescence probe integrated polymer nanoparticles for sensing biological thiol molecules. Scientific Reports, 2014, 4, 7057.	3.3	30
330	Selfâ€Assembled Single‧ite Nanozyme for Tumor‧pecific Amplified Cascade Enzymatic Therapy. Angewandte Chemie, 2021, 133, 3038-3044.	2.0	30
331	Rationally "clicked―post-modification of a highly stable metal–organic framework and its high improvement on CO2-selective capture. RSC Advances, 2013, 3, 15566.	3.6	29
332	One-Pot Synthesis of Antitumor Agent PMX 610 by a Copper(II)-Incorporated Mesoporous Catalyst. ACS Sustainable Chemistry and Engineering, 2014, 2, 934-941.	6.7	29
333	Doxorubicin‣oaded Metal–Organic Gels for pH and Glutathione Dualâ€Responsive Release. ChemNanoMat, 2016, 2, 504-508.	2.8	29
334	Disruption of dual homeostasis by a metal-organic framework nanoreactor for ferroptosis-based immunotherapy of tumor. Biomaterials, 2022, 284, 121502.	11.4	29
335	The construction of a supramolecular polymeric rotaxane from bipyridine-ruthenium and cyclodextrin. Chemical Communications, 2005, , 1702.	4.1	28
336	Surface Conductive Grapheneâ€Wrapped Micromotors Exhibiting Enhanced Motion. Small, 2015, 11, 5023-5027.	10.0	28
337	Crystal Multiâ€Conformational Control Through Deformable Carbonâ€Sulfur Bond for Singletâ€Triplet Emissive Tuning. Angewandte Chemie, 2019, 131, 4372-4377.	2.0	28
338	Enhancing the Solubility and Transdermal Delivery of Drugs Using Ionic Liquidâ€Inâ€Oil Microemulsions. Advanced Functional Materials, 2021, 31, 2102794.	14.9	28
339	Missingâ€Linkerâ€Assisted Artesunate Delivery by Metal–Organic Frameworks for Synergistic Cancer Treatment. Angewandte Chemie - International Edition, 2021, 60, 26254-26259.	13.8	28
340	A bistable pretzelane. Chemical Communications, 2009, , 4844.	4.1	27
341	Drug Encapsulation and Release by Mesoporous Silica Nanoparticles: The Effect of Surface Functional Groups. Chemistry - A European Journal, 2014, 20, 11276-11282.	3.3	27
342	<i>In Situ</i> Integration of Anisotropic SnO <sub>2</sub> Heterostructures inside Three-Dimensional Graphene Aerogel for Enhanced Lithium Storage. ACS Applied Materials & Interfaces, 2015, 7, 26085-26093.	8.0	27

#	Article	IF	CITATIONS
343	Controlled Movement of Cucurbiturils in Host–Guest Systems. ChemPlusChem, 2017, 82, 30-41.	2.8	27
344	Uncovering the Design Principle of Amino Acid-Derived Photoluminescent Biodots with Tailor-Made Structure–Properties and Applications for Cellular Bioimaging. ACS Applied Materials & Interfaces, 2018, 10, 19881-19888.	8.0	27
345	Crossâ€Linked Polyphosphazene Hollow Nanosphereâ€Derived N/Pâ€Doped Porous Carbon with Single Nonprecious Metal Atoms for the Oxygen Reduction Reaction. Angewandte Chemie, 2020, 132, 14747-14754.	2.0	27
346	Ultrastable Tb-Organic Framework as a Selective Sensor of Phenylglyoxylic Acid in Urine. ACS Applied Materials & Interfaces, 2021, 13, 33546-33556.	8.0	27
347	Albumin-Based Therapeutics Capable of Glutathione Consumption and Hydrogen Peroxide Generation for Synergetic Chemodynamic and Chemotherapy of Cancer. ACS Nano, 2022, 16, 2319-2329.	14.6	27
348	Biocompatible Twoâ€Photon Absorbing Dipyridyldiketopyrrolopyrroles for Metalâ€Ionâ€Mediated Selfâ€Assembly Modulation and Fluorescence Imaging. Advanced Optical Materials, 2016, 4, 746-755.	7.3	26
349	Morphology Tuning of Self-Assembled Perylene Monoimide from Nanoparticles to Colloidosomes with Enhanced Excimeric NIR Emission for Bioimaging. ACS Applied Materials & Interfaces, 2016, 8, 2336-2347.	8.0	26
350	Reduction-Responsive Carbon Dots for Real-Time Ratiometric Monitoring of Anticancer Prodrug Activation in Living Cells. ACS Biomaterials Science and Engineering, 2017, 3, 1535-1541.	5.2	26
351	NIR-absorbing dye functionalized hollow mesoporous silica nanoparticles for combined photothermal–chemotherapy. Chemical Communications, 2017, 53, 12032-12035.	4.1	26
352	Tuning interfacial sequence between nitrogen-doped carbon layer and Au nanoparticles on metal-organic framework-derived TiO2 to enhance photocatalytic hydrogen production. Chemical Engineering Journal, 2020, 397, 125468.	12.7	26
353	Tumor-targeted upconverting nanoplatform constructed by host-guest interaction for near-infrared-light-actuated synergistic photodynamic-/chemotherapy. Chemical Engineering Journal, 2020, 390, 124516.	12.7	26
354	Molecular Binding Behavior of Pyridine-2,6-dicarboxamide-Bridged Bis(β-cyclodextrin) with Oligopeptides:  Switchable Molecular Binding Mode. Bioconjugate Chemistry, 2004, 15, 300-306.	3.6	25
355	Dual-responsive drug release from oligonucleotide-capped mesoporous silica nanoparticles. Biomaterials Science, 2013, 1, 912.	5.4	25
356	Photopolymerization of Diacetylene on Aligned Multiwall Carbon Nanotube Microfibers for High-Performance Energy Devices. ACS Applied Materials & Interfaces, 2016, 8, 32643-32648.	8.0	25
357	Two-dimensional C <sub>60</sub> nano-meshes <i>via</i> crystal transformation. Nanoscale, 2019, 11, 8692-8698.	5.6	25
358	Significantly enhanced photocatalytic performance of In <sub>2</sub> O <sub>3</sub> hollow spheres <i>via</i> the coating effect of an N,S-codoped carbon layer. Journal of Materials Chemistry A, 2019, 7, 25423-25432.	10.3	25
359	Inverse Evolution of Helicity from the Molecular to the Macroscopic Level Based on <i>N</i> -Terminal Aromatic Amino Acids. ACS Nano, 2021, 15, 5322-5332.	14.6	25
360	Binding Behavior of Aliphatic Oligopeptides by Bridged and Metallobridged Bis(β-cyclodextrin)s Bearing an Oxamido Bis(2-benzoic) Carboxyl Linker. Bioconjugate Chemistry, 2004, 15, 1236-1245.	3.6	24

#	Article	IF	CITATIONS
361	Nanoarchitectures Constructed from Resulting Polypseudorotaxanes of theβ-Cyclodextrin/4,4'-Dipyridine Inclusion Complex with Co2+and Zn2+Coordination Centers. Chemistry of Materials, 2006, 18, 4423-4429.	6.7	24
362	Poly(Acrylic Acid)â€Capped and Dyeâ€Loaded Graphene Oxideâ€Mesoporous Silica: A Nanoâ€Sandwich for Twoâ€Photon and Photoacoustic Dualâ€Mode Imaging. Particle and Particle Systems Characterization, 2014, 31, 1060-1066.	2.3	24
363	Near-IR squaraine dye–loaded gated periodic mesoporous organosilica for photo-oxidation of phenol in a continuous-flow device. Science Advances, 2015, 1, e1500390.	10.3	24
364	Oxidation-triggered aggregation of gold nanoparticles for naked-eye detection of hydrogen peroxide. Chemical Communications, 2016, 52, 3508-3511.	4.1	24
365	Controllable synthesis of Ce-doped α-MnO <sub>2</sub> for low-temperature selective catalytic reduction of NO. Catalysis Science and Technology, 2017, 7, 1565-1572.	4.1	24
366	Effect of Carbazolyl Groups on Photophysical Properties of Cyanuric Chloride. ACS Applied Materials & Interfaces, 2019, 11, 47162-47169.	8.0	24
367	Bacteria Inspired Internal Standard SERS Substrate for Quantitative Detection. ACS Applied Bio Materials, 2021, 4, 2009-2019.	4.6	24
368	Waterâ€Induced Blueâ€Green Variable Nonconventional Ultralong Room Temperature Phosphorescence from Crossâ€Linked Copolymers via Click Chemistry. Advanced Optical Materials, 2021, 9, 2101284.	7.3	24
369	Directing the Architecture of Surface-Clean Cu <sub>2</sub> 0 for CO Electroreduction. Journal of the American Chemical Society, 2022, 144, 12410-12420.	13.7	24
370	Multi[2]rotaxanes with Gold Nanoparticles as Centers. Organic Letters, 2006, 8, 1267-1270.	4.6	23
371	Larger ï€-extended anti-/syn-aroylenediimidazole polyaromatic compounds: synthesis, physical properties, self-assembly, and quasi-linear conjugation effect. RSC Advances, 2014, 4, 17822-17831.	3.6	23
372	Controlled synthesis of concave cuboctahedral nitrogen-rich metal–organic framework nanoparticles showing enhanced catalytic activation of epoxides with carbon dioxide. CrystEngComm, 2015, 17, 8596-8601.	2.6	23
373	Scalable Synthesis of Honeycomblike V <sub>2</sub> O <sub>5</sub> /Carbon Nanotube Networks as Enhanced Cathodes for Lithium-Ion Batteries. ACS Applied Materials & Interfaces, 2017, 9, 42438-42443.	8.0	23
374	Recognition-Induced Supramolecular Porous Nanosphere Formation from Cyclodextrin Conjugated by Cholic Acid. Langmuir, 2006, 22, 3434-3438.	3.5	22
375	Inclusion Behavior of βâ€Cyclodextrin with Bipyridine Molecules: Factors Governing Hostâ€Guest Inclusion Geometries. Chemistry - an Asian Journal, 2009, 4, 446-456.	3.3	22
376	A quinoxaline based N-heteroacene interfacial layer for efficient hole-injection in quantum dot light-emitting diodes. Nanoscale, 2015, 7, 11531-11535.	5.6	22
377	A Novel Strategy for the Construction of Covalent Organic Frameworks from Nonporous Covalent Organic Polymers. Angewandte Chemie, 2019, 131, 4960-4964.	2.0	22
378	NIRâ€Lightâ€Activated Combination Therapy with a Precise Ratio of Photosensitizer and Prodrug Using a Host–Guest Strategy. Angewandte Chemie, 2019, 131, 7723-7728.	2.0	22

#	Article	IF	CITATIONS
379	Impeding Catalyst Sulfur Poisoning in Aqueous Solution by Metal–Organic Framework Composites. Small Methods, 2020, 4, 1900890.	8.6	22
380	Simple Vanilla Derivatives for Long-Lived Room-Temperature Polymer Phosphorescence as Invisible Security Inks. Research, 2021, 2021, 8096263.	5.7	22
381	Bioresorbable Scaffolds with Biocatalytic Chemotherapy and In Situ Microenvironment Modulation for Postoperative Tissue Repair. Advanced Functional Materials, 2021, 31, 2008732.	14.9	22
382	Effects of Hydrophobicity on Antimicrobial Activity, Selectivity, and Functional Mechanism of Guanidiniumâ€Functionalized Polymers. Advanced Healthcare Materials, 2022, 11, e2100482.	7.6	22
383	Mechanosynthesis of Higherâ€Order Cocrystals: Tuning Order, Functionality and Size in Cocrystal Design**. Angewandte Chemie - International Edition, 2021, 60, 17481-17490.	13.8	22
384	ç´«å¤å‰æį€æ´»æœ‰æœºåºå^å^†å掺æ <del>,</del> èšå•̂物体系的é•;å⁻¿å¹½å®æ¸©ç£·å‰. Science China Materia	ıls,623022, 6	552 <b>2</b> 160-216
385	New challenge of metal–organic frameworks for high-efficient separation of hydrogen chloride toward clean hydrogen energy. Journal of Materials Chemistry A, 2015, 3, 5275-5279.	10.3	21
386	Structural Engineering of Luminogens with High Emission Efficiency Both in Solution and in the Solid State. Angewandte Chemie, 2019, 131, 11541-11545.	2.0	21
387	Construction of a Sandwiched MOF@COF Composite as a Size-Selective Catalyst. Cell Reports Physical Science, 2020, 1, 100272.	5.6	21
388	Spinel-Oxide-Integrated BiVO <sub>4</sub> Photoanodes with Photothermal Effect for Efficient Solar Water Oxidation. ACS Applied Materials & amp; Interfaces, 2021, 13, 48901-48912.	8.0	21
389	Distinct interpenetrated metal–organic frameworks constructed from crown ether-based strut analogue. CrystEngComm, 2013, 15, 841-844.	2.6	20
390	{[M(NH3)6][Ag4M4Sn3Se13]}â^ž (M=Zn, Mn): Three-dimensional chalcogenide frameworks constructed from quaternary metal selenide clusters with two different transition metals. Journal of Solid State Chemistry, 2014, 218, 146-150.	2.9	20
391	β-Diketimine appended periodic mesoporous organosilica as a scaffold for immobilization of palladium acetate: An efficient green catalyst for Wacker type reaction. Journal of Catalysis, 2014, 318, 43-52.	6.2	20
392	Graphene Oxide Wrapping of Gold–Silica Core–Shell Nanohybrids for Photoacoustic Signal Generation and Bimodal Imaging. ChemNanoMat, 2015, 1, 39-45.	2.8	20
393	Remarkable Vapochromic Behavior of Pure Organic Octahedron Embedded in Porous Frameworks. Small, 2016, 12, 3302-3308.	10.0	20
394	Carbon Dioxide Capture: Covalent Organic Frameworks for CO <sub>2</sub> Capture (Adv. Mater.) Tj ETQq0 0 C	) rgBT/Ove 21.0	erlock 10 Tf 5

395	An oxaliplatin( <scp>iv</scp> ) prodrug-based supramolecular self-delivery nanocarrier for targeted colorectal cancer treatment. Chemical Communications, 2018, 54, 12762-12765.	4.1	20
396	Charge separation in hybrid metal–organic framework films for enhanced catalytic CO <sub>2</sub> conversion. Journal of Materials Chemistry A, 2021, 9, 2694-2699.	10.3	20

#	Article	IF	CITATIONS
397	Hybrid Nanoparticles as Drug Carriers for Controlled Chemotherapy of Cancer. Chemical Record, 2016, 16, 1833-1851.	5.8	19
398	Ordered Single-Crystalline Anatase TiO <sub>2</sub> Nanorod Clusters Planted on Graphene for Fast Charge Transfer in Photoelectrochemical Solar Cells. Small, 2017, 13, 1700793.	10.0	19
399	Efficient Production of Reactive Oxygen Species from Fe <sub>3</sub> O <sub>4</sub> /ZnPC Coloaded Nanoreactor for Cancer Therapeutics In Vivo. Small Structures, 2020, 1, 2000065.	12.0	19
400	Boosting the stability and photoelectrochemical activity of a BiVO <sub>4</sub> photoanode through a bifunctional polymer coating. Journal of Materials Chemistry A, 2021, 9, 3309-3313.	10.3	19
401	K+-Intercalated carbon nitride with electron storage property for high-efficiency visible light driven nitrogen fixation. Chemical Engineering Journal, 2022, 433, 133573.	12.7	19
402	Highly Effective Photocatalytic Radical Reactions Triggered by a Photoactive Metal–Organic Framework. ACS Applied Materials & Interfaces, 2022, 14, 23518-23526.	8.0	19
403	Organic Anion Recognition of Naphthalenesulfonates by Steroid-Modifiedβ-Cyclodextrins: Enhanced Molecular Binding Ability and Molecular Selectivity. Journal of Organic Chemistry, 2006, 71, 6010-6019.	3.2	18
404	Synthesis of Ag2S quantum dots by a single-source precursor: an efficient electrode material for rapid detection of phenol. Analytical Methods, 2014, 6, 2059.	2.7	18
405	Selfâ€Assembly of Organic Building Blocks with Directly Exfoliated Graphene to Fabricate Di―and Tricomponent Hybrids. ChemNanoMat, 2015, 1, 517-527.	2.8	18
406	Anionic polymer as a quasi-neutral medium for low-cost synthesis of titanosilicate molecular sieves in the presence of high-concentration alkali metal ions. Journal of Catalysis, 2016, 338, 321-328.	6.2	18
407	Troponate/Aminotroponate Ruthenium–Arene Complexes: Synthesis, Structure, and Ligand-Tuned Mechanistic Pathway for Direct C–H Bond Arylation with Aryl Chlorides in Water. Inorganic Chemistry, 2016, 55, 6739-6749.	4.0	18
408	Modular Molecular Selfâ€Assembly for Diversified Chiroptical Systems. Small, 2020, 16, 2002036.	10.0	18
409	Hierarchical nano-to-molecular disassembly of boron dipyrromethene nanoparticles for enhanced tumor penetration and activatable photodynamic therapy. Biomaterials, 2021, 275, 120945.	11.4	18
410	A Photoswitchable [2]Rotaxane Array on Graphene Oxide. Asian Journal of Organic Chemistry, 2012, 1, 314-318.	2.7	17
411	Nanonet as a scaffold with targeted functionalities. Journal of Materials Chemistry, 2012, 22, 24983.	6.7	17
412	Iron(III)â€Quantityâ€Dependent Aggregation–Dispersion Conversion of Functionalized Gold Nanoparticles. Chemistry - A European Journal, 2014, 20, 4032-4037.	3.3	17
413	A novel inhaled multi-pronged attack against respiratory bacteria. European Journal of Pharmaceutical Sciences, 2015, 70, 37-44.	4.0	17
414	Remarkable colorimetric sensing of heavy metal ions based on thiol-rich nanoframes. Chemical Communications, 2016, 52, 13691-13694.	4.1	17

#	Article	IF	CITATIONS
415	A New Era of Metal–Organic Framework Nanomaterials and Applications. ACS Applied Nano Materials, 2020, 3, 4917-4919.	5.0	17
416	A three-photon probe with dual emission colors for imaging of Zn( <scp>ii</scp> ) ions in living cells. Chemical Communications, 2014, 50, 14378-14381.	4.1	16
417	Aggregation-induced chiral symmetry breaking of a naphthalimide–cyanostilbene dyad. Physical Chemistry Chemical Physics, 2014, 16, 23854-23860.	2.8	16
418	An amine functionalized rht-type metal-organic framework with the improved performance for gas uptake. Inorganic Chemistry Communication, 2014, 46, 13-16.	3.9	16
419	Waterâ€Bindingâ€Mediated Gelation/Crystallization and Thermosensitive Superchirality. Angewandte Chemie, 2018, 130, 7900-7905.	2.0	16
420	Understanding the Pathway of Gas Hydrate Formation with Porous Materials for Enhanced Gas Separation. Research, 2019, 2019, 3206024.	5.7	16
421	Cyclodextrin-Based [1]Rotaxanes on Gold Nanoparticles. International Journal of Molecular Sciences, 2012, 13, 10132-10142.	4.1	15
422	Solvothermal syntheses of three new one-dimensional ternary selenidostannates: [DBNH][M1/2Sn1/2Se2] (M=Mn, Zn, Hg). Journal of Solid State Chemistry, 2013, 204, 86-90.	2.9	15
423	An rht-type metal–organic framework constructed from an unsymmetrical ligand exhibiting high hydrogen uptake capability. RSC Advances, 2014, 4, 53975-53980.	3.6	15
424	Superior optical nonlinearity of an exceptional fluorescent stilbene dye. Applied Physics Letters, 2015, 106, .	3.3	15
425	Dual Fluorescence-Activated Study of Tumor Cell Apoptosis by an Optofluidic System. IEEE Journal of Selected Topics in Quantum Electronics, 2015, 21, 392-398.	2.9	15
426	Tailored Antibiotic Combination Powders for Inhaled Rotational Antibiotic Therapy. Journal of Pharmaceutical Sciences, 2016, 105, 1501-1512.	3.3	15
427	Bioinspired Antimicrobial Nanodots with Amphiphilic and Zwitterionic-like Characteristics for Combating Multidrug-Resistant Bacteria and Biofilm Removal. ACS Applied Nano Materials, 2018, 1, 2062-2068.	5.0	15
428	Engineering Migration Pathway for Effective Separation of Photogenerated Carriers on Multicomponent Heterojunctions Coated with Nitrogenâ€Đoped Carbon. Chemistry - A European Journal, 2019, 25, 14133-14139.	3.3	15
429	Carbene atalyzed Enantioselective Aldol Reaction: Postâ€Aldol Stereochemistry Control and Formation of Quaternary Stereogenic Centers. Angewandte Chemie - International Edition, 2021, 60, 159-165.	13.8	15
430	Tumor Microenvironment Activated Chemodynamic–Photodynamic Therapy by Multistage Selfâ€Assembly Engineered Protein Nanomedicine. Advanced Functional Materials, 2022, 32, .	14.9	15
431	Phonon Energy Transfer in Graphene–Photoacid Hybrids. Journal of Physical Chemistry C, 2012, 116, 4175-4181.	3.1	14
432	Steroid-Decorated Antibiotic Microparticles for Inhaled Anti-Infective Therapy. Journal of Pharmaceutical Sciences, 2014, 103, 1115-1125.	3.3	14

#	Article	IF	CITATIONS
433	A concise method to prepare novel fused heteroaromatic diones through double Friedel–Crafts acylation. Organic Chemistry Frontiers, 2014, 1, 391-394.	4.5	14
434	A topologically substituted boron nitride hybrid aerogel for highly selective CO2 uptake. Nano Research, 2018, 11, 6325-6335.	10.4	14
435	Porous catalytic membranes for CO2 conversion. Journal of Energy Chemistry, 2021, 63, 74-86.	12.9	14
436	Hybrid Carbon Dot Assembly as a Reactive Oxygen Species Nanogenerator for Ultrasound-Assisted Tumor Ablation. Jacs Au, 2021, 1, 2328-2338.	7.9	14
437	NIR-Light-Intensified Hypoxic Microenvironment for Cascaded Supra-Prodrug Activation and Synergistic Chemo/Photodynamic Cancer Therapy. , 2022, 4, 111-119.		14
438	Critical involvement of lysyl oxidase in seizure-induced neuronal damage through ERK-Alox5-dependent ferroptosis and its therapeutic implications. Acta Pharmaceutica Sinica B, 2022, 12, 3513-3528.	12.0	14
439	Construction of Covalentâ€Organic Frameworks (COFs) from Amorphous Covalent Organic Polymers via Linkage Replacement. Angewandte Chemie, 2019, 131, 17843-17847.	2.0	13
440	Research progress in endogenous H <sub>2</sub> Sâ€activatable nanoplatforms for cancer theranostics. View, 2020, 1, e15.	5.3	13
441	A Robust Aluminum Metal-Organic Framework with Temperature-Induced Breathing Effect. , 2020, 2, 220-226.		13
442	Multidimensional Structure Conformation of Persulfurated Benzene for Highly Efficient Phosphorescence. ACS Applied Materials & Interfaces, 2021, 13, 1314-1322.	8.0	13
443	Waterâ€Soluble Doublyâ€Strapped Isolated Perylene Diimide Chromophore. Angewandte Chemie - International Edition, 2022, 61, .	13.8	13
444	Photothermal-responsive [2]rotaxanes. RSC Advances, 2013, 3, 2341.	3.6	12
445	Crystalline Li3V6O16 rods as high-capacity anode materials for aqueous rechargeable lithium batteries (ARLB). RSC Advances, 2014, 4, 28601-28605.	3.6	12
446	Titanium(IV) in the Organicâ€Structureâ€Directingâ€Agentâ€Free Synthesis of Hydrophobic and Largeâ€Pore Molecular Sieves as Redox Catalysts. ChemSusChem, 2015, 8, 2476-2480.	6.8	12
447	Two metal–organic frameworks sharing the same basic framework show distinct interpenetration degrees and different performances in CO <sub>2</sub> catalytic conversion. CrystEngComm, 2017, 19, 4157-4161.	2.6	12
448	Self-Assembly of <i>N</i> -Terminal Aryl Amino Acids into Adaptive Single- and Double-Strand Helices. Journal of Physical Chemistry Letters, 2020, 11, 4147-4155.	4.6	12
449	Fourâ€inâ€One Stimulusâ€Responsive Longâ€Lived Luminescent Systems Based on Pyreneâ€Doped Amorphous Polymers. Angewandte Chemie, 2022, 134, .	2.0	12
450	An imine-based approach to prepare amine-functionalized Janus gold nanoparticles. Chemical Communications, 2015, 51, 11622-11625.	4.1	11

#	Article	IF	CITATIONS
451	A Threeâ€Photon Active Organic Fluorophore for Deep Tissue Ratiometric Imaging of Intracellular Divalent Zinc. Chemistry - an Asian Journal, 2016, 11, 1523-1527.	3.3	11
452	Preparation of Ultrathin Twoâ€Ðimensional Ti <sub><i>x</i></sub> Ta <sub>1â^'<i>x</i></sub> S <sub><i>y</i></sub> O <sub><i>z</i></sub> Nanosheets as Highly Efficient Photothermal Agents. Angewandte Chemie, 2017, 129, 7950-7954.	2.0	11
453	Solvent―and HFâ€Free Synthesis of Flexible Chromiumâ€Based MILâ€53 and MILâ€88B. ChemNanoMat, 2020, 6 204-207.	6, <sub>2.8</sub>	11
454	Aromatic vapor responsive molecular packing rearrangement in supramolecular gels. Materials Chemistry Frontiers, 2020, 4, 2452-2461.	5.9	11
455	Self-assembled semiconducting polymer based hybrid nanoagents for synergistic tumor treatment. Biomaterials, 2021, 279, 121188.	11.4	11
456	Synthesis of Some Selenacrown Ethers and the Thermodynamic Origin of Their Complexation with C60. Journal of Inclusion Phenomena and Macrocyclic Chemistry, 2005, 51, 191-198.	1.6	10
457	Synthesis and in vitro evaluation of charge reversal photoresponsive quinoline tethered mesoporous silica for targeted drug delivery. Journal of Materials Chemistry B, 2014, 2, 7971-7977.	5.8	10
458	Quantum dot decorated aligned carbon nanotube bundles for a performance enhanced photoswitch. Nanoscale, 2016, 8, 8547-8552.	5.6	10
459	The fabrication of LiMn2O4 and Na1.16V3O8 based full cell aqueous rechargeable battery to power portable wearable electronics devices. Materials and Design, 2016, 93, 291-296.	7.0	10
460	Colour-tunable ultra-long emission. Nature Photonics, 2019, 13, 373-375.	31.4	10
461	Toward miniaturizing microelectronics using covalent organic framework dielectric. Matter, 2021, 4, 1760-1762.	10.0	10
462	Solid-state structures and superstructures of two charged donor–acceptor rotaxanes. Tetrahedron Letters, 2011, 52, 2044-2047.	1.4	9
463	Rational Design and Synthesis of a Highly Porous Copperâ€Based Interpenetrated Metal–Organic Framework for High CO <sub>2</sub> and H <sub>2</sub> Adsorption. ChemPlusChem, 2015, 80, 1259-1266.	2.8	9
464	Intracellular Reductionâ€Responsive Sheddable Copolymer Micelles for Targeted Anticancer Drug Delivery. Asian Journal of Organic Chemistry, 2015, 4, 226-232.	2.7	9
465	Constructing Synergetic Trilayered TiO <sub>2</sub> Photoanodes Based on a Flexible Nanotube Array/Ti Substrate for Efficient Solar Cells. ChemNanoMat, 2017, 3, 58-64.	2.8	9
466	Self-Assembly Evolution of <i>N</i> -Terminal Aromatic Amino Acids with Transient Supramolecular Chirality. Journal of Physical Chemistry Letters, 2020, 11, 1490-1496.	4.6	9
467	Self-assembly behavior of inclusion complex formed by b-cyclodextrin with a-aminopyridine. Science in China Series B: Chemistry, 2004, 47, 200.	0.8	8
468	A layered liquid crystalline droplet. Journal of Materials Chemistry, 2009, 19, 3469.	6.7	8

#	Article	IF	CITATIONS
469	The photoirradiation induced p–n junction in naphthylamine-based organic photovoltaic cells. Nanoscale, 2015, 7, 14612-14617.	5.6	8
470	Facile fabrication of concave cubic nitrogen-rich metal–organic framework nanocrystals for gas uptake. CrystEngComm, 2016, 18, 1277-1281.	2.6	8
471	MAPKK Inhibitor U0126 Inhibits <i>Plasmodiophora brassicae</i> Development. Phytopathology, 2018, 108, 711-720.	2.2	8
472	Carbonâ€Dotâ€Mediated Coâ€Administration of Chemotherapeutic Agents for Reversing Cisplatin Resistance in Cancer Therapy. ChemNanoMat, 2018, 4, 801-806.	2.8	8
473	Selfâ€5orting Doubleâ€Network Hydrogels with Tunable Supramolecular Handedness and Mechanical Properties. Angewandte Chemie, 2019, 131, 9466-9472.	2.0	8
474	Folic acid functionalized hollow nanoparticles for selective photodynamic therapy of cutaneous squamous cell carcinoma. Materials Chemistry Frontiers, 2019, 3, 1113-1122.	5.9	8
475	Photoinduced Radical Emission in a Coassembly System. Angewandte Chemie, 2021, 133, 24035.	2.0	8
476	Thiolate-Assisted Route for Constructing Chalcogen Quantum Dots with Photoinduced Fluorescence Enhancement. ACS Applied Materials & Interfaces, 2021, 13, 48449-48456.	8.0	8
477	Room Temperature Phosphorescence: Achieving Amorphous Ultralong Room Temperature Phosphorescence by Coassembling Planar Small Organic Molecules with Polyvinyl Alcohol (Adv.) Tj ETQq1 1 0.78	4311149rgBT	⁻/Øverlock 1
478	NIRâ€Actuated Remote Activation of Ferroptosis in Target Tumor Cells through a Photothermally Responsive Ironâ€Chelated Biopolymer Nanoplatform. Angewandte Chemie, 2021, 133, 9020-9029.	2.0	7
479	Synthesis of novel indolyl modified β-cyclodextrins and their molecular recognition behavior controlled by the solution's pH value. Perkin Transactions II RSC, 2002, , 463-469.	1.1	6
480	Self-assembly behavior of phenyl modified β-cyclodextrins. Science in China Series B: Chemistry, 2006, 49, 230-237.	0.8	6
481	Rigidityâ^'Stability Relationship in Interlocked Model Complexes Containing Phenylene-Ethynylene-Based Disubstituted Naphthalene and Benzene. Crystal Growth and Design, 2009, 9, 2300-2309.	3.0	6
482	Encapsulation of CdSe/ZnS nanocrystals within mesoporous silica spheres. Materials Research Bulletin, 2013, 48, 1530-1535.	5.2	6
483	Synthesis and application of polyacrylic acid-based nanoparticles for photodynamic therapy. Journal of Controlled Release, 2015, 213, e20-e21.	9.9	6
484	An iGlu Receptor Antagonist and Its Simultaneous Use with an Anticancer Drug for Cancer Therapy. Chemistry - A European Journal, 2015, 21, 6123-6131.	3.3	6
485	Organic Nanoparticle-Based Fluorescent Chemosensor for Selective Switching ON and OFF of Photodynamic Therapy (PDT). ChemistrySelect, 2016, 1, 6523-6531.	1.5	6
486	Perylenetetracarboxylic–metal assemblies and anisotropic charge transport in a Cu <sup>II</sup> assembly. Nanoscale, 2016, 8, 9134-9140.	5.6	6

#	Article	IF	CITATIONS
487	Optically Induced Structural Instability in Gold–Silica Nanostructures: A Case Study. Journal of Physical Chemistry C, 2016, 120, 11230-11236.	3.1	6
488	Smart Therapeutics Achieved via Host–Guest Assemblies. , 2017, , 391-420.		6
489	ZIF-8 Nanoparticles for Facile Processing into Useful Fabric Composites. ACS Applied Nano Materials, 2021, 4, 6562-6567.	5.0	6
490	A Plasmonic Supramolecular Nanohybrid as a Contrast Agent for Site‣elective Computed Tomography Imaging of Tumor. Advanced Functional Materials, 2022, 32, 2110575.	14.9	6
491	Chiral molecular nanosilicas. Chemical Science, 2022, 13, 4029-4040.	7.4	6
492	One-Dimensional Helical Aggregates Organized from Achiral Imine-Based Polymers. , 2022, 4, 715-723.		6
493	Nanosystems for Immune Regulation against Bacterial Infections: A Review. ACS Applied Nano Materials, 2022, 5, 13959-13971.	5.0	6
494	Cation-exchange resin towards low-cost synthesis of high-performance TS-1 zeolites in the presence of alkali-metal ions. RSC Advances, 2016, 6, 15615-15621.	3.6	5
495	Preparation of Responsive Carbon Dots for Anticancer Drug Delivery. Methods in Molecular Biology, 2019, 2000, 227-234.	0.9	5
496	A glucose-depleting silica nanosystem for increasing reactive oxygen species and scavenging glutathione in cancer therapy. Chemical Communications, 2019, 55, 13374-13377.	4.1	5
497	Multifunctional Nanosystems with Enhanced Cellular Uptake for Tumor Therapy. Advanced Healthcare Materials, 2022, 11, e2101703.	7.6	5
498	Synergistic Assembly of Covalent and Supramolecular Polymers. Macromolecular Rapid Communications, 2016, 37, 920-923.	3.9	4
499	Graphene-Based Materials in Biosensing, Bioimaging, and Therapeutics. Carbon Nanostructures, 2016, , 35-61.	0.1	4
500	Light intensity field enhancement (LIFE) induced localized edge abrasion of silica-coated silver nanoprisms. Nanoscale, 2017, 9, 15356-15361.	5.6	4
501	Inhaled non-steroidal polyphenolic alternatives for anti-inflammatory combination therapy. Powder Technology, 2018, 339, 244-255.	4.2	4
502	Ultrathin Supramolecular Architectures Self-Assembled from a <i>C</i> <sub>3</sub> -Symmetric Synthon for Selective Metal Binding. ACS Applied Materials & Interfaces, 2020, 12, 9673-9681.	8.0	4
503	Dual Gateâ€Controlled Therapeutics for Overcoming Bacteriumâ€Induced Drug Resistance and Potentiating Cancer Immunotherapy. Angewandte Chemie, 2021, 133, 14132-14140.	2.0	4
504	Macrocycle-Based Metal–Organic Frameworks with NO <sub>2</sub> -Driven On/Off Switch of Conductivity. ACS Applied Materials & Interfaces, 2021, 13, 27066-27073.	8.0	4

#	Article	IF	CITATIONS
505	Film-facilitated formation of ferrocenecarboxylic acid-embedded metal-organic framework nanoparticles for sonodynamic osteosarcoma treatment. Materials Today Chemistry, 2022, 24, 100842.	3.5	4

Imaging: Upconversion Nanoparticles as a Contrast Agent for Photoacoustic Imaging in Live Mice (Adv.) Tj ETQq0 0.0 rgBT /Oyerlock 10 506

507	Carbeneâ€Catalyzed Enantioselective Aldol Reaction: Postâ€Aldol Stereochemistry Control and Formation of Quaternary Stereogenic Centers. Angewandte Chemie, 2021, 133, 161-167.	2.0	3
508	Elucidating the anticancer activities of guanidinium-functionalized amphiphilic random copolymers by varying the structure and composition in the hydrophobic monomer. Theranostics, 2021, 11, 8977-8992.	10.0	3
509	Supramolecular Assemblies from Pillararenes (Micellar, Vesicular and Tubular Formations). Monographs in Supramolecular Chemistry, 2015, , 208-228.	0.2	3
510	Molecular self-assembly behavior of mono[6-O-6-(4-carboxyl-phenyl)]-β-CD in solution and solid state. Science Bulletin, 2003, 48, 1535-1538.	1.7	2
511	Byproduct-induced in-situ formation of gold colloidal superparticles. Science China Materials, 2015, 58, 860-866.	6.3	2
512	Semiconducting polymer dots with phosphorescent Ir(III)-complex for photodynamic cancer therapy. Journal of Controlled Release, 2015, 213, e43.	9.9	2
513	Aqueous assembly. Nature Chemistry, 2015, 7, 944-945.	13.6	2
514	Metal-Organic Frameworks: Bimetallic Metal-Organic Frameworks: Probing the Lewis Acid Site for CO2Conversion (Small 17/2016). Small, 2016, 12, 2386-2386.	10.0	2
515	Recent Research Advancements in NO-Releasing Nanomaterials. Wuli Huaxue Xuebao/ Acta Physico - Chimica Sinica, 2017, 33, 903-917.	4.9	2
516	Mechanosynthesis of Higherâ€Order Cocrystals: Tuning Order, Functionality and Size in Cocrystal Design**. Angewandte Chemie, 2021, 133, 17622-17631.	2.0	2
517	Missingâ€Linkerâ€Assisted Artesunate Delivery by Metalâ€Organic Frameworks for Synergistic Cancer Treatment. Angewandte Chemie, 0, , .	2.0	2
518	Schottky Contacts Regularized Linear Regression for Signal Inconsistency Circumvent in Resistive Gas Microâ€Nanosensors. Small Methods, 2021, 5, e2101194.	8.6	2
519	Waterâ€Soluble Doublyâ€Strapped Isolated Perylene Diimide Chromophore. Angewandte Chemie, 0, , .	2.0	2
520	Molecular Recognition Thermodynamics of Steroids by Novel Oligo(aminoethylamino)-?-cyclodextrins Bearing Anthryl: Enhanced Molecular Binding Ability by Co-inclusion Complexation. Journal of Inclusion Phenomena and Macrocyclic Chemistry, 2004, 50, 3-11.	1.6	1
521	Drug Delivery: Functional Silica Nanoparticles for Redoxâ€Triggered Drug/ssDNA Coâ€delivery (Adv.) Tj ETQq1 1	0.784314 7.6	rgBT /Ov
599	Delivery of polyamine-functionalized mesoporous silica nanoparticles into cancerous cells. Journal	0.0	1

522 of Controlled Release, 2015, 213, e100.

#	Article	IF	CITATIONS
523	Nanomaterial-Based Drug Delivery Carriers for Cancer Therapy. SpringerBriefs in Applied Sciences and Technology, 2017, , .	0.4	1
524	Nanomaterial-Based Drug Delivery Carriers for Cancer Therapy. SpringerBriefs in Applied Sciences and Technology, 2017, , 15-54.	0.4	1
525	Solar Cells: Ordered Single-Crystalline Anatase TiO <sub>2</sub> Nanorod Clusters Planted on Graphene for Fast Charge Transfer in Photoelectrochemical Solar Cells (Small 28/2017). Small, 2017, 13,	10.0	1
526	In Vivo Near-Infrared Fluorescence Imaging. , 2018, , 67-125.		1
527	Efficient Nobleâ€Metalâ€Free Catalysts Supported by Threeâ€Dimensional Ordered Hierarchical Porous Carbon. Chemistry - an Asian Journal, 2020, 15, 2513-2519.	3.3	1
528	Molecular Expansion for Constructing Porous Organic Polymers with High Surface Areas and Wellâ€Defined Nanopores. Angewandte Chemie, 2020, 132, 19655-19661.	2.0	1
529	Molecular self-assembly behavior of mono[6-O-6-(4-carboxyl-phenyl)]-b-CD in solution and solid state. Science Bulletin, 2003, 48, 1535.	1.7	1
530	Lightâ€Triggered Hypoxiaâ€Responsive Nanoscale Metalâ€Organic Frameworks for Highly Efficient Antitumor Treatment. Advanced Optical Materials, 0, , 2201043.	7.3	1
531	Mesoporous carbon nanomaterial prepared directly by the second-side modified cyclodextrin through silica as template. Journal of Chemical Research, 2004, 2004, 533-535.	1.3	0
532	Cancer Treatment: Ultrasmall Phosphorescent Polymer Dots for Ratiometric Oxygen Sensing and Photodynamic Cancer Therapy (Adv. Funct. Mater. 30/2014). Advanced Functional Materials, 2014, 24, 4822-4822.	14.9	0
533	Frontispiece: Rational Design and Synthesis of a Highly Porous Copper-Based Interpenetrated Metal-Organic Framework for High CO2and H2Adsorption. ChemPlusChem, 2015, 80, n/a-n/a.	2.8	0
534	Metallic and Upconversion Nanoparticles as Photoacoustic Contrast Agents for Biomedical Imaging. , 2016, , 1199-1222.		0
535	Separation of Light Hydrocarbons by Metal-Organic Frameworks. Series on Chemistry, Energy and the Environment, 2018, , 247-280.	0.3	0
536	Responsive Supramolecular Vesicles Based on Host-Guest Recognition for Biomedical Applications. , 2019, , 1-25.		0
537	Frontispiece: Diverse Role of Solvents in Controlling Supramolecular Chirality. Chemistry - A European Journal, 2019, 25, .	3.3	0
538	Frontispiece: Self‧orting Doubleâ€Network Hydrogels with Tunable Supramolecular Handedness and Mechanical Properties. Angewandte Chemie - International Edition, 2019, 58, .	13.8	0
539	Frontispiz: Selfâ€Sorting Doubleâ€Network Hydrogels with Tunable Supramolecular Handedness and Mechanical Properties. Angewandte Chemie, 2019, 131, .	2.0	0
540	Frontispiece: Amorphous Ionic Polymers with Colorâ€Tunable Ultralong Organic Phosphorescence. Angewandte Chemie - International Edition, 2019, 58, .	13.8	0

#	Article	IF	CITATIONS
541	Frontispiz: Amorphous Ionic Polymers with Colorâ€Tunable Ultralong Organic Phosphorescence. Angewandte Chemie, 2019, 131, .	2.0	0
542	Metallic and Upconversion Nanoparticles as Photoacoustic Contrast Agents for Biomedical Imaging. , 2015, , 1-24.		0
543	Responsive Supramolecular Vesicles Based on Host-Guest Recognition for Biomedical Applications. , 2020, , 1413-1437.		0